28th DOE/NRC Nuclear Air Cleaning and Treatment Conference

EFFICIENCY OF HEPA FILTERS IN MULTI-STAGE FILTER SYSTEMS

Werner Bergman, Consultant
PO Box 451
Pleasanton, CA 94566
wernerbergman@comcast.net

ABSTRACT

This report examines the efficiency of HEPA filters in multi-stage HEPA filter systems. For heterodisperse aerosols, the particle removal efficiency decreases with increasing filter stage due to the decreasing average size of the aerosols at each filter stage. This experimentally observed phenomenon is consistent with a constant HEPA filter efficiency for each filter stage. However, a number of experimental observations of decreasing aerosol removal efficiency with increasing filter stage have been used to infer that the HEPA filter efficiency decreases with increasing filter stage. This report examines these experimental observations and demonstrates that the apparent decrease in HEPA filter efficiency is an artifact of the measurement and is due to background interference. The source of this artifact is the background aerosol concentration relative to the aerosol concentration that penetrates the HEPA filter. When the background is properly accounted, the efficiency of the HEPA filter does not change with each stage of filtration. A theory of filter efficiency measurements with background concentrations is developed and is in agreement with the experimental measurements.

I. INTRODUCTION

A number of studies infer that the efficiency of HEPA filters in a multi-stage filtration system decreases with increasing filter stage (1-4). This decrease in filter efficiency is in addition to the decrease in particle collection efficiency due to heterodisperse aerosols. For heterodisperse aerosols, the average particle size decreases with increasing filtration stage and thus shows a lower particle collection efficiency. This decreased particle collection efficiency does not imply a lower filter efficiency as will be shown in the next section. The smaller particle size follows the filter efficiency curve, which has a lower efficiency for smaller particle sizes until a minimum efficiency is reached at the most penetrating particle size. Further decrease in particle size will result in increasing particle collection efficiency.

Ryan et al (1,2) suggest the mechanism for the lower filter efficiency in higher filter stages is a percolation of deposited radioactive particles through the filter media due to alpha recoil during radioactive decay. Other proposed mechanisms for the higher efficiency in the initial stages of HEPA filters are due to the increased particle concentration filling up holes in the media or particle coagulation to form larger particles and hence higher efficiency (4). As the particle concentration decreases in the

subsequent filter stages , these mechanisms are not significant and yield an apparent lower filter efficiency.

The perceived decrease in HEPA filter efficiencies for higher filter stages has been incorporated into guidance documents for analyzing release of radioactive material from non-reactor nuclear facilities. Elder et al (5) recommends that the first stage HEPA filter be credited with an efficiency of 99.9% and each subsequent stage with 99.8%. These data are not based on experimental measurements, but are obtained from the expert opinions of twelve participants at a meeting held in 1971 (6). The Elder report is currently used as the assumed HEPA filter efficiencies under accident conditions in the Safety Anaysis Reports for the plutonium facilities at the Lawrence Livermore National Laboratory and the Los Alamos National Laboratory. Walker (7) recommends efficiencies of 99.9% for the first stage, 99.0% for the second and third stages, and 83% for the fourth stage based on experimental measurements.

We will show that the decreased filter efficiency for higher filter stages is due to the background aerosols that create artifacts in the filter efficiency. When the background aerosols are properly accounted, the HEPA filter efficiency in the higher stages is the same as in the first stage.

II. HETERODISPERSE AEROSOLS HAVE LOWER COLLECTION EFFICIENCY AT HIGHER FILTER STAGES

The aerosol collection efficiency for heterodisperse aerosols will decrease with increasing HEPA filter stage because of the HEPA filtration curve. Figure 1 shows a graph of the percent filter penetration as a function of aerosol diameter for a standard nuclear grade, 1000 cfm HEPA filter with aluminum separators (8). The HEPA filter is tested using heterodisperse dioctyl sebacate (DOS) aerosols generated using a Laskin nozzle genertor. The aerosol size distribution is measured before and after the filter using a Particle Measuring System, HS-LAS laser particle counter. The challenge aerosol is diluted by a factor of 1000 to prevent coincidence counting. The ratio of the downstream to upstream (after correcting for dilution) concentrations is used to compute the percent penetration. The experimental data is fitted to a log-normal distribution function with Dg=0.172 and SDg=1.61 (9). The HEPA filter penetration curve in Figure 1 shows a size interval in which a greater fraction of aerosols having diameters within that interval can pass. The further the particle size lies outside of this interval, the greater the particle removal efficiency.

We can illustrate how heterodisperse aerosols have lower particle removal efficiencies for increasing stages of HEPA filter with the examples shown in Figures 2-5. Figure 2 shows a series of aerosol size distributions beginning with the initial aerosol entering the series of HEPA filters and the resulting size distributions after the first, second, third and fourth HEPA filter. The initial aerosol has a log-normal size distribution with a mass median aerodynamic diameter (MMAD) of 1 um and a geometric standard deviation (SDg) of 2

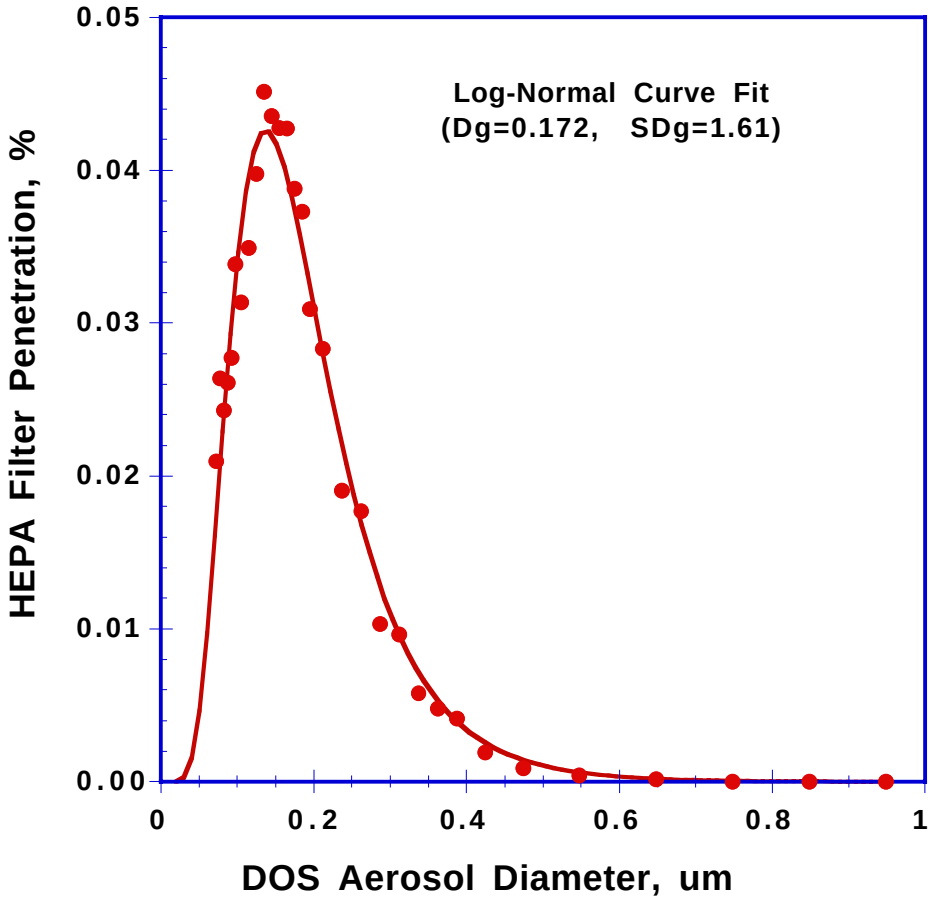

Figure 1. Percent filter penetration of a typical,1000 cfm,deep-pleated, nuclear grade HEPA filter with aluminum separators as a function of aerosol diameter (8).

The equation for the aerosol mass distribution as a function of aerosol diameter after the nth HEPA filter is given by

$$dm_n = \frac{M_n}{\sqrt{2\pi}\, D \ln(SD_{gn})} e^{-\frac{1}{2}\left(\frac{\ln(D/MMAD_n)}{\ln(SDgn)}\right)^2} dD \qquad (1)$$

where dm_n = differential aerosol mass concentration in size interval dD, g/ $m^3/\mu m$

M_n = integrated aerosol mass concentration after nth HEPA filter, g/m^3

D = aerosol diameter, μm

$MMAD_n$ = mass median aerodynamic diameter of aerosol after nth HEPA filter, μm

SD_{ng} = geometric standard deviation of aerosol after nth HEPA filter

Equation 1 is also used to fit the filter penetration data from Figure 1 to the log-normal size distribution after substituting Dg for MMAD (9).

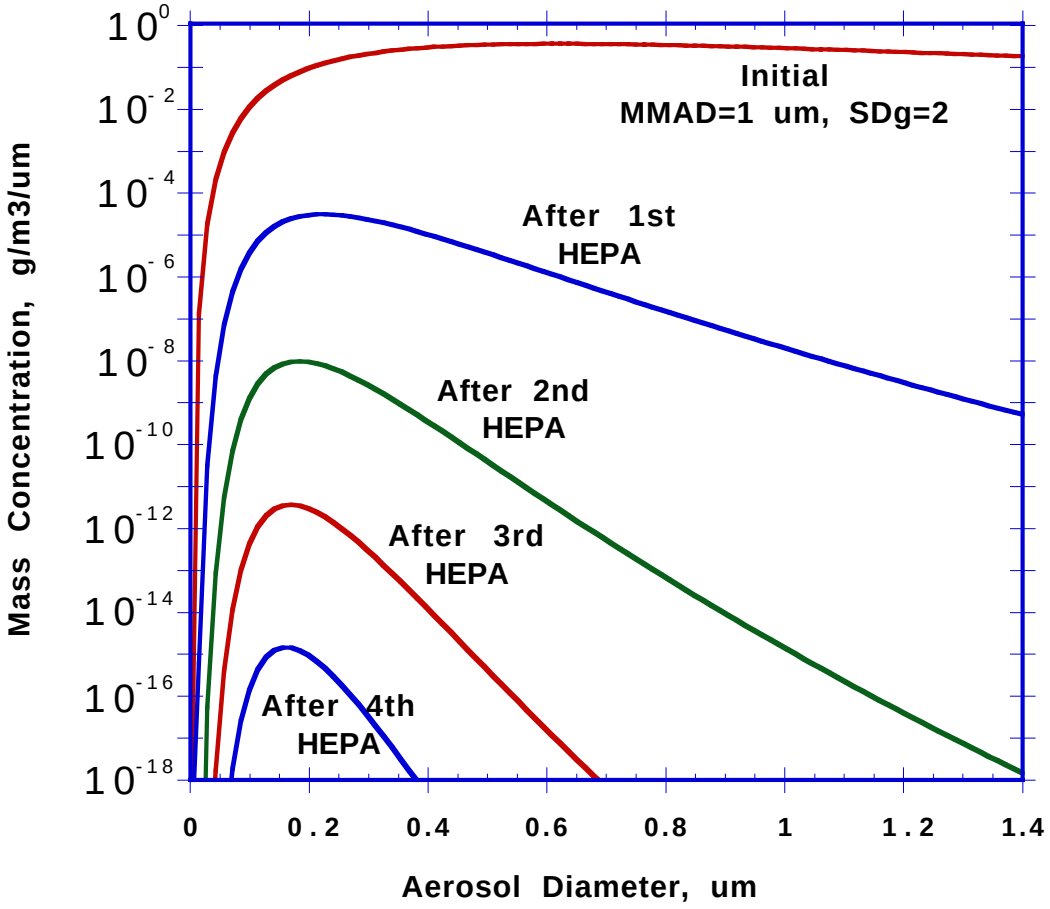

Figure 2. Graph of the aerosol mass concentration as a function of particle size for the initial aerosol and for the aerosol after passing through the 1st, 2nd, 3rd, and 4th HEPA filters, where the HEPA filter curve is given in Figure 1.

The curve in Figure 2 for the initial aerosol was generated using Equation 1 with MMAD = 1μm and SDg=2. The concentration data in Figure 2 is plotted on a log scale to fit all of the curves on a single chart. The curve showing the aerosol distribution after the first HEPA filter is computed by multiplying the data from the initial distribution by the HEPA penetration data in Figure 1. Each subsequent curve is generated from the preceding curve by multiplying by the HEPA penetration data in Figure 1 as shown in Equation 2.

$$m_n(MMAD_n, SD_{gn}, D) = \left(P(D)\right)^n m_0(MMAD_0, SD_{g0}, D) \qquad (2)$$

where $m_n(MMAD_n, SD_{gn}, D)$ = mass aerosol distribution after the nth HEPA filter and given by Equation 1

$P(D)$ = HEPA filter penetration curve from Figure 1

$M_0(MMAD_0, SD_{g0}, D)$ = initial mass aerosol distribution

n = number of HEPA filters aerosol penetrated

The curves in Figure 2 show that the large particles are selectively removed with each pass through a HEPA filter yielding a more narrow aerosol size distribution and shifted to smaller sizes. This effect can be better seen in Figure 3 where the concentration curves are normalized to fit on a linear scale. The penetration curve for the HEPA filter from Figure 1 is also added in Figure 3. Note that the linear concentration curves in Figure 3 show the size distributions much better than log concentration curves in Figure 2.

Figure 3 shows the initial aerosol concentration has a relatively broad size distribution. After passing through the first HEPA filter, the aerosol size distribution has become more narrow and shifted dramatically to smaller sizes. The change in the aerosol size distribution occurs because the HEPA filter allows only a small portion of the smaller particles from the original size distribution to pass through the filter. The shift in the aerosol size distribution after passing the second and third HEPA filter is less pronounced.

Figure 4 shows a graph of MMAD and SDg of three initially different size distributions as the aerosols pass through four stages of HEPA filtration. The most dramatic change in the aerosol size distribution occurs after the first HEPA filter. It is clear from Figure 4 that all of the initially different aerosol size distributions converge to the same size distributions after passing through the first and each subsequent HEPA filter.

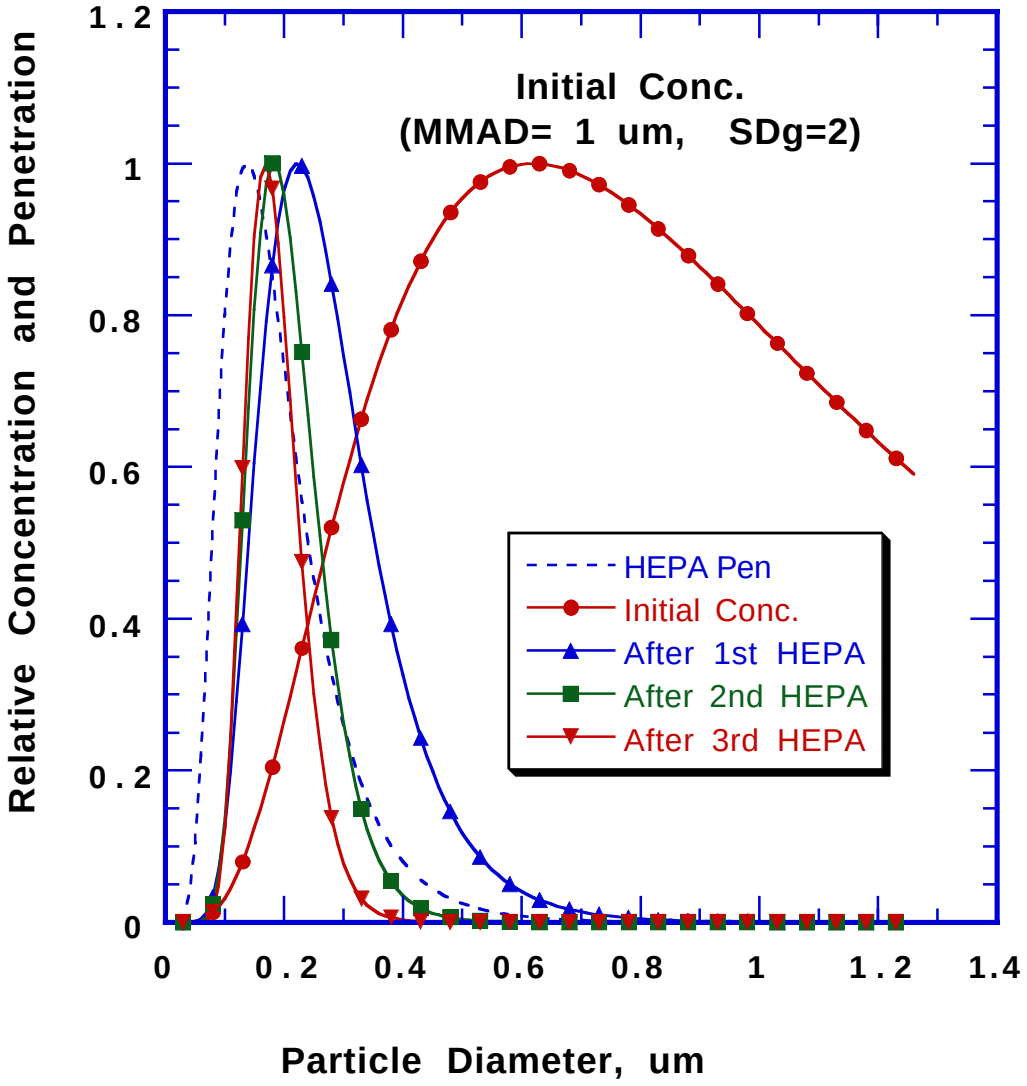

Figure 3. Aerosol concentration curves from Figure 2 normalized to fit on a linear graph. The HEPA filter penetration curve from Figure 1 is also normalized and added here.

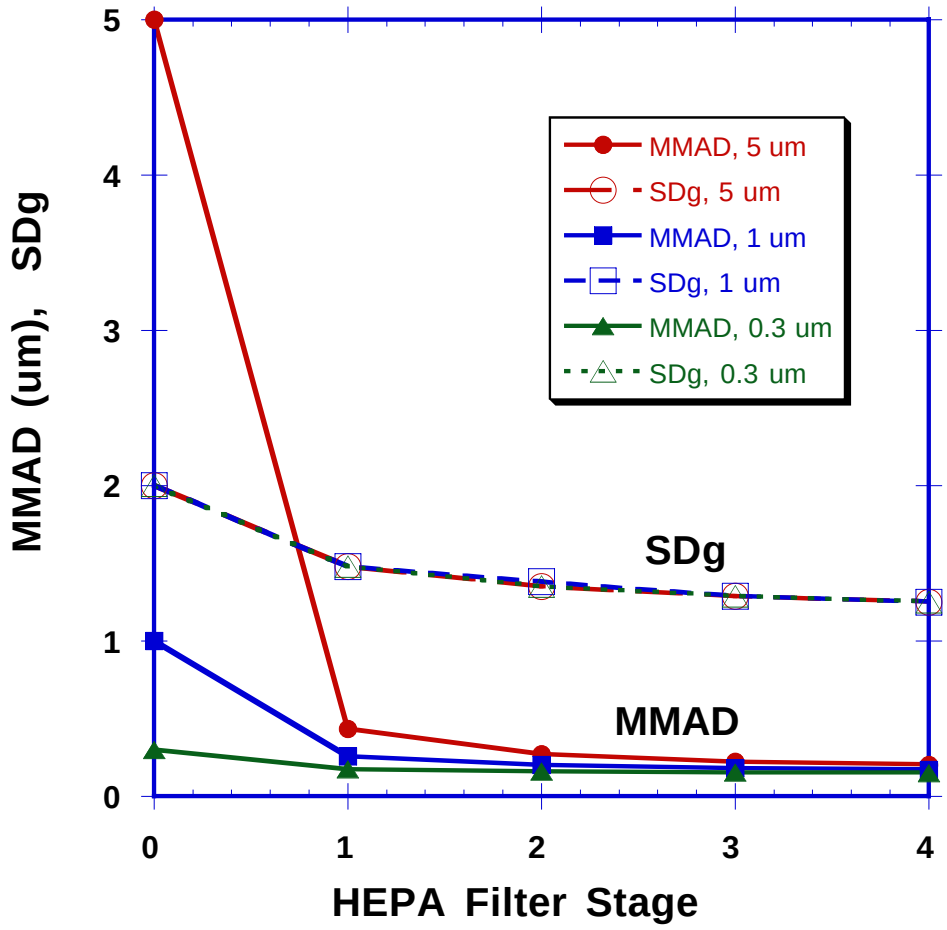

Figure 4. Variation in the median size (MMAD) and width (SDg) of three different aerosol distributions passing through four stages of HEPA filtration. The aerosol distributions are taken from Figure 3.

The efficiency of aerosol removal will vary with each filter stage because the aerosol size distribution changes after each stage as shown in Figure 5. The efficiency for aerosol removal, E_{An}, is computed from Equation 3.

$$E_{An} = 100\% \left(1 - \frac{M_n}{M_{n-1}} \right) \qquad (3)$$

Where M_n and M_{n-1} are the integrated mass concentrations after the nth and n-1th HEPA filter and are obtained from Equation 1.

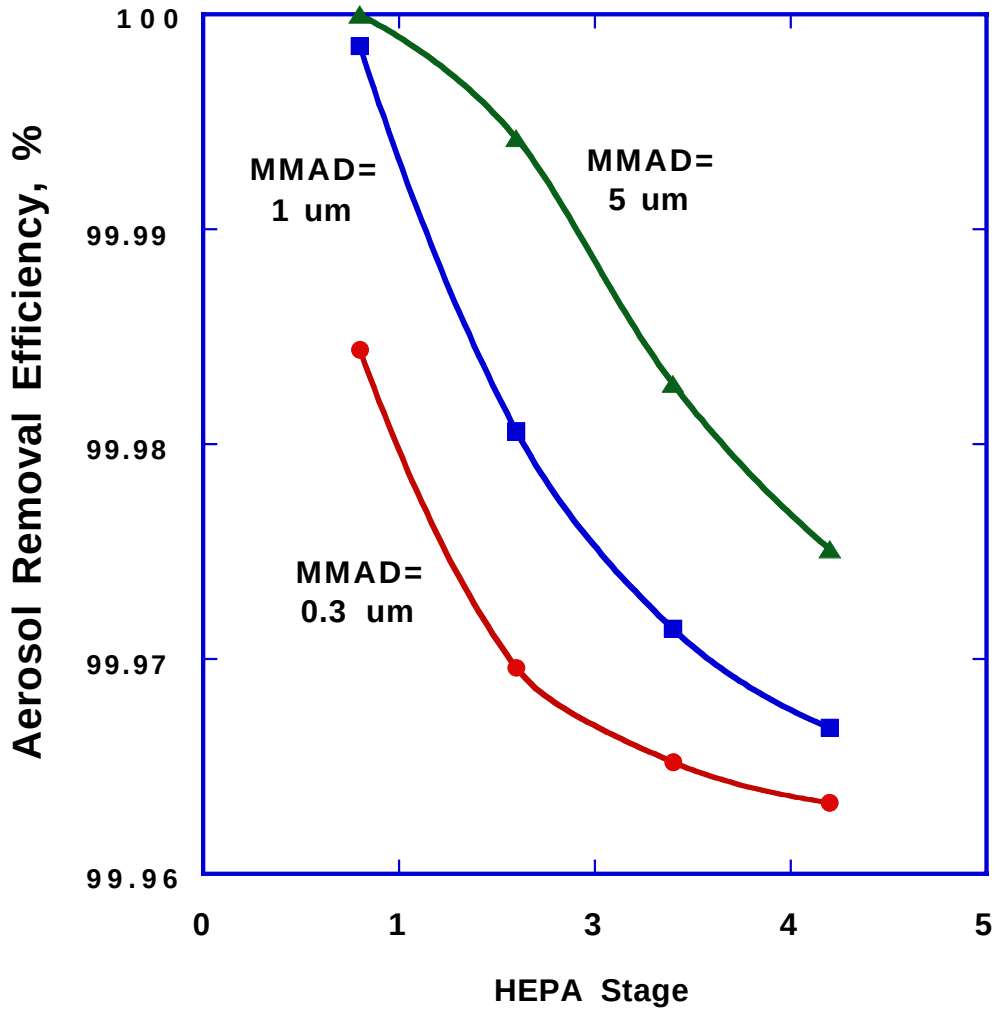

Figure 5. Aerosol removal efficiency for three different size distributions at increasing stages of HEPA filter filtration.

Note that the HEPA filter efficiency is constant at each stage and is shown in Figure 1. The aerosol removal efficiency decreases with increasing HEPA stage because the aerosol size distribution shifts to the most penetrating particle size in the HEPA filtration curve in Figure 1

.

III. EXPERIMENTAL DATA SUGGESTS THAT HIGHER STAGE HEPA FILTERS HAVE LOWER EFFICIENCIES

In addition to the effect shown in the previous section, where heterodisperse aerosols have lower efficiency with increasing HEPA filter stage, researchers suggest that the HEPA filter efficiency also decreases with increasing filter stage. Ryan et al measures the total activity on the four stages of HEPA filters at a plutonium processing plant using scintillation counting (1). The results of their measurements are shown in Table 1. The efficiency of the first filter is very high. However, the efficiency of the following filters becomes progressively worse and far less than expected for the HEPA filter. Ryan et al use this data as an indication of the alpha recoil process causing increased penetration of the HEPA filter.

Table 1. Activity measurements on 4 stages of 1,000 cfm sized HEPA filters that are exposed to 239Pu exhaust using scintillation counting. Ryan et al (1).

Filter Stage.	Exposure time, months	Activity, counts/min/in^2	Filter efficiency, %
1	35	552,000	99.9998%
2	35	0.89	76.1%
3	35	0.154	55.0**%**
4	35	0.126	---
1	27	22,949	99.998%
2	27	0.549	96.7%
3	27	0.0144	76.6%
4	27	0.0044	----

Hetland and Russel report that the HEPA filter efficiency for the higher stages in a multi-stage filtration system at the Rocky Flats Plant is significantly lower than the efficiency of the first HEPA filter (3). Table 2 shows the filter efficiency of the fourth stage HEPA filter is only 84%.

Table 2. HEPA filter performance data from Rocky Flats Pu processing plant, (3)

Filter Stage	Exposure, days	Challenge Conc. mCi/ml	Efficiency, %
1	90	8.0×10^{-7}	99.8 (est.) [1]
2	90	1.6 x 10-9 (est.)[1]	99.5 (est.) [1]
3	90	9.9×10^{-13} (comp)[2]	94
4	90	6.0×10^{-14}	83

[1] Based on division of 99.999% efficiency between first and second stage.

[2] Computed based on an air dilution factor of 8.1 between the second and third stages.

One of the major arguments supporting the concept of alpha recoil causing enhanced filter penetrations is the decrease in measured efficiency in the higher stages of a multi-stage HEPA filter system as shown in Figure 6. We plot the efficiency of each filter in a multi-stage filter system as a function of filter stage. The results for the data from Ryan et al in Table 1 for 239Pu are plotted along with the 238Pu data from McDowell et al (2) and the 239Pu field data in Table 2 from Hetland and Russell (3). Note that since Hetland and Russell (3) do not provide the filter efficiency for filter stages 1 and 2 separately, but give the efficiency for the combined stages 1 and 2 as 99.999%, we arbitrarily assign an efficiency of 99.8% for the first and 99.5% for the second. Although the data by McDowell generally follows the trend of lower efficiency with increasing filter stage, there are several exceptions. These are presumably due to the high uncertainty with the low counts.

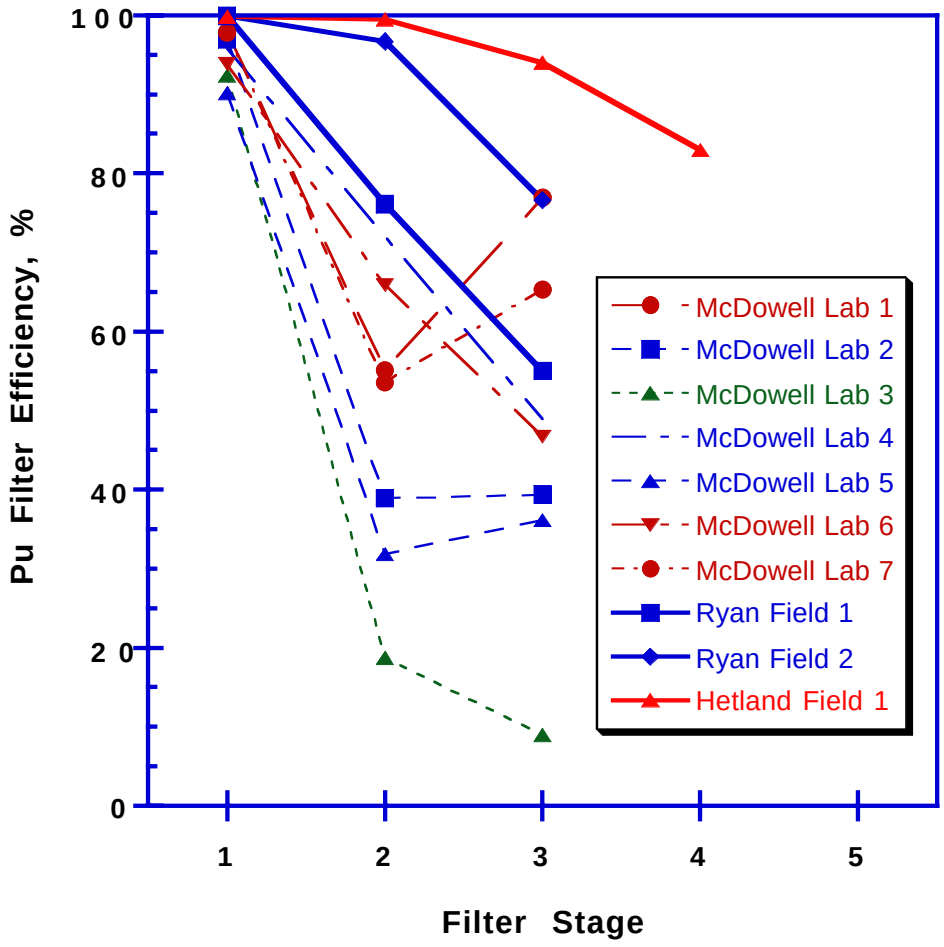

Figure 6. Efficiency on each filter stage of a multistage filter test system as a function of filter stage for 238Pu (McDowell et al) and 239Pu (Ryan et al and Hettland et al). (1-3)

According to the alpha recoil hypothesis, the higher filtration stages will experience a greater decrease in filter efficiency because the transmitted alpha recoil fragments represent a larger fraction of the material deposited on the filter than the lower filtration stages.

Thus the experimental data used to support the alpha recoil hypothesis can be viewed as lower efficiency for the higher filtration stages as in Figure 6 or as higher efficiency for filter stages with higher activity (or conversely higher filter challenge concentration) as in Figure 7. According to the alpha recoil hypothesis, these observations are due to the formation of recoil fragments and the transmission of these fragments through the filter media by subsequent recoils or from thermal resuspensions. The alternative explanation for the experimental data in Figures 6 and 7 is the presence of background contamination. Without additional information, both explanations agree with the experimental measurements.

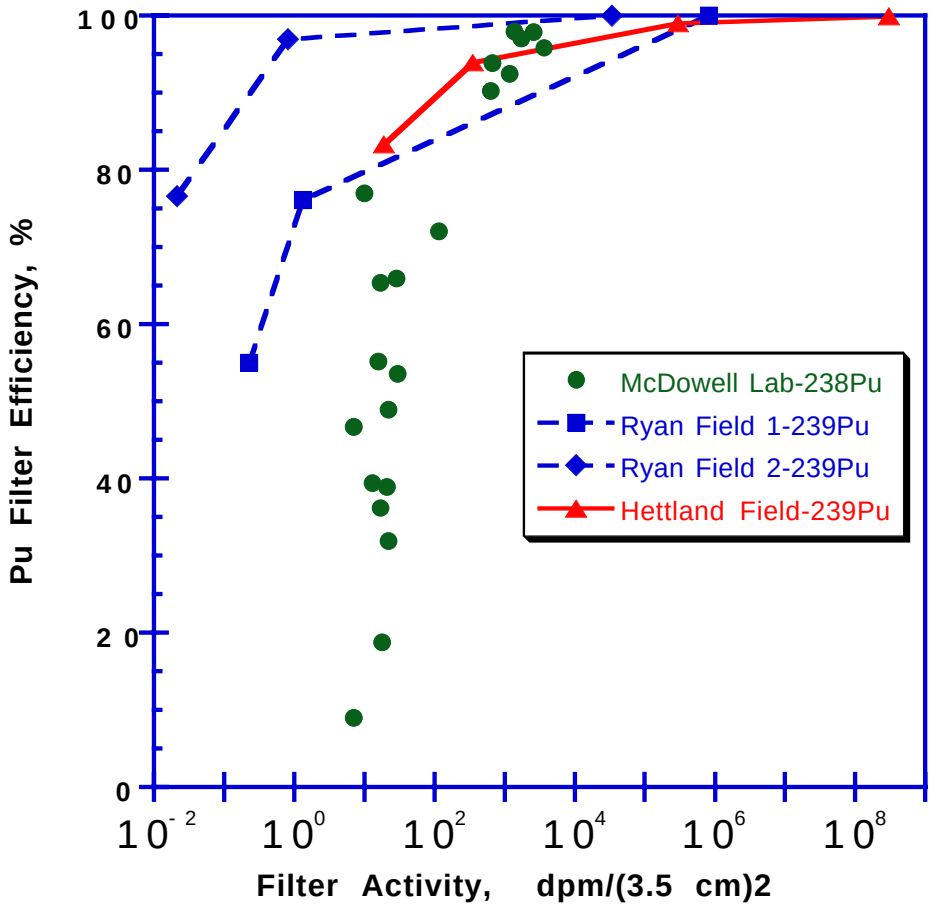

Figure 7. Efficiency on each filter stage of a multistage filter test system as a function of filter activity for 238Pu and 239Pu. The activity from the field data is normalized to compare directly with the 3.5 cm diameter filters used in McDowell's lab studies (1-3)

IV ANALYSIS OF LOW EFFICIENCIES FOR SECONDARY FILTERS IN MULTI-STAGE FILTRATION SYSTEMS SUGGEST THE CAUSE IS DUE TO LEAKS AND BACKGROUND INTERFERENCE

A review of the literature show very few studies of the efficiency of HEPA filters under field conditions. Among the few studies are those by Hetland and Russel (Table 2) and the data compiled by Ryan et al (Table 1). Additional studies are given below.

Carbaugh conducts a survey of HEPA filter experience and finds that for a three year period from 1977-1979, 58% of all filters are changed out and 12% of the filters are replaced due to filter failures.(10) The following rates are observed for the filters that are changed out: 63% for high pressure drop, 15% for leak test failure, 13% for preventative maintenance, 5% for suspected damage, 4% for radiation build up and 1% unspecified (10). Of the 12% filter failures, the following frequencies and failure modes are identified: 64% unknown cause, 19% handling or installation damage, 6% frame failure, 6% gasket or seal failure, and 5% media rupture.

Frigerio and Stowe evaluates the radioactive emissions from various U.S. nuclear facilities and finds enhanced emissions are due to outright filter failures, excessive moisture, material hold up in ducts, cross contamination of ducts and HEPA frames during filter changes (4). They find that, on average, the total releases due to these occurrences are about 20 times the release of the system operating at its baseline value. If we assume that a two stage HEPA filter has a combined efficiency of 99.9998% under accident conditions (99.9% for stage one and 99.8% for stage two) as recommended by Elder et al (5), applying the factor of 20 for the field experience would yield an average lifetime efficiency of 99.996%. If we apportion this effective lifetime system efficiency equally between the two HEPA filter stages, we have 99.4% efficiency for each filter stage. Note that this approximation includes both the reduced efficiency from accidents (Elder et al 5) and from lifetime operating experiences, including filter failure (Frigerio and Stowe, 4). This is a conservative estimate because it assumes the HEPA filtration system is under accident conditions throughout its life (i.e. 99.9% for stage one and 99.8% for stage two).

Figure 8 shows the monthly alpha particulate release from a mixed oxide (PuO_2, UO_2) fuel fabrication facility during its life operation (4). The curve in Figure 8 is due primarily to Pu releases because its activity is much higher than that of U. The peaks at 28 and 53 months were due to HEPA filter failures. The peak at 47 months is due to excessive moisture which causes the soluble plutonium and uranium salts from a scrap recovery run to penetrate through the filter and become airborne on the other side. Several of the other smaller peaks in Figure 8 are also due to moisture carry over. The three major peak emissions represent 73% of the total life emissions while all of the excursions represent 95% of the total emissions.

Removing the moisture would have a major reduction in emissions. Frigerio and Stowe recommended using a prefilter composed of Soda Lime to remove moisture and acid and

prevent the penetration of soluble salts through the HEPA filter. The alkaline prefilter would convert the plutonium and uranium salts to insoluble oxides and hydroxides and is amenable to recovery and recycling of the plutonium and uranium.

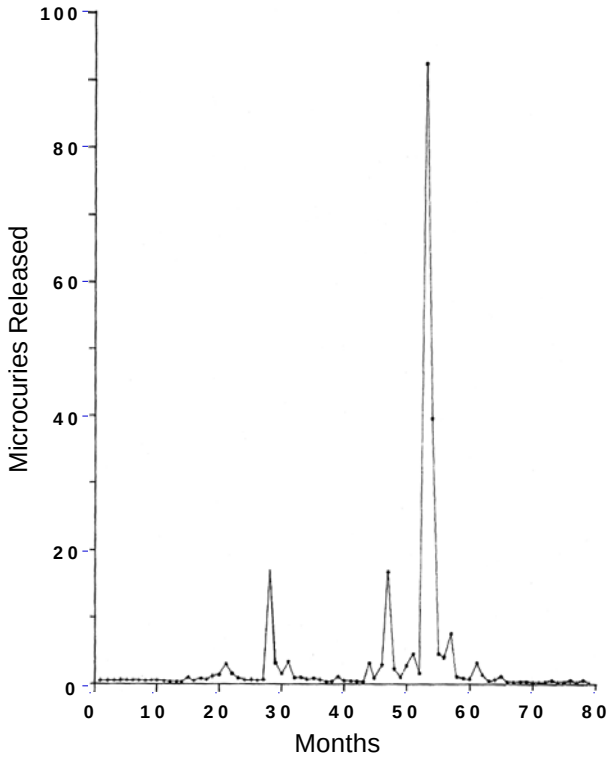

Figure 8. Alpha particle release history of a mixed oxide fuel fabrication facility The peaks at 28 and 53 months were due to HEPA filter failures. The remaining peaks are primarily due to high moisture conditions that allowed soluble Pu and U salts to penetrate the HEPA filters (Frigerio and Stowe 4)

Water accumulation on HEPA filters can result in significant increases in filter penetration even without soluble particles. Bergman et al show that the percent DOP penetration for 0.3 μm diameter particles increases in direct proportion to the relative pressure drop increase from the collected water according to Equation 4 (11).

$$P = 1.3\, P_0\, \Delta P/\Delta P_0 \qquad (4)$$

where P = penetration of water loaded HEPA filter, %

P_0 = initial dry filter penetration, %

ΔP = pressure drop of water loaded HEPA filter, inches water

ΔP_0 = pressure drop of dry HEPA filter, inches water

Other studies show that volatile acids and moisture can penetrate multiple HEPA filters and condense on a downstream HEPA filter. Woodard et al (12) find significant amount of nitrates on the sixth stage HEPA filter in a Pu acid recovery operation. Although no radioactive particles are found on the filter, the HEPA filter gains 20 pounds after one year of use. The nitric acid fumes and water forms nitrates on the asbestos separators. The added deposits do not affect the final filter efficiency which is measured at 99.996% (initial is 99.994%) using the standard 0.3 μm DOP test. Since the asbestos fiber media used in the HEPA filter is resistant to acid attack, the glass fiber media used in current HEPA filters may show signs of degradation with the acid exposure. No information was presented on the pressure drop, but considering that the acid vapor is deposited on the separators, the increase is expected to be minimal.

Frigerio and Stowe also find that after a filter failure or other significant release, the release rate from the third stage HEPA filter decays slowly with a half life of 3 weeks to several months (4). They confirm that the slow release is due to holdup of Pu in the ducts by gamma ray location along the ducts, bends and crevices.

A noteworthy observation in the Frigerio and Stowe study is their finding that the observed HEPA filter penetration decreases with increasing challenge concentration as shown in Figure 9 (4). This data is similar to the data in Figure 7 that is used to support the hypothesis of alpha recoil causing enhanced filter penetration. (Note that the data in Figure 7 is in efficiency and not penetration as in Figure 9. The curve in Figure 7 showing increasing efficiency with increasing challenge concentration when re-plotted as penetration will show decreasing penetration with increasing challenge concentration and thus be in agreement with Figure 9.) The data in Figure 9 is obtained from measuring the transient concentrations in Figure 8 at weekly and sometimes daily intervals for each of the two HEPA filter stages in order to obtain the large range in challenge concentrations. They are not able to explain their findings but speculate the findings are due to either plugging of holes in the HEPA filter at higher concentrations or increased particle coagulation at the higher concentrations which increases the particle size and consequently filter efficiency. Both speculations are not correct. Plugging holes results in a permanent filter improvement and hence will not show a consistent trend in the penetration verses concentration curves. Once the holes are plugged, lower concentrations will also show a low penetration as would higher concentrations. The coagulation hypothesis is potentially credible for the first stage HEPA filter but not the remaining stages since the first stage HEPA filter will remove any particle size increases due to coagulation and therefore not affect the remaining HEPA filter stages.

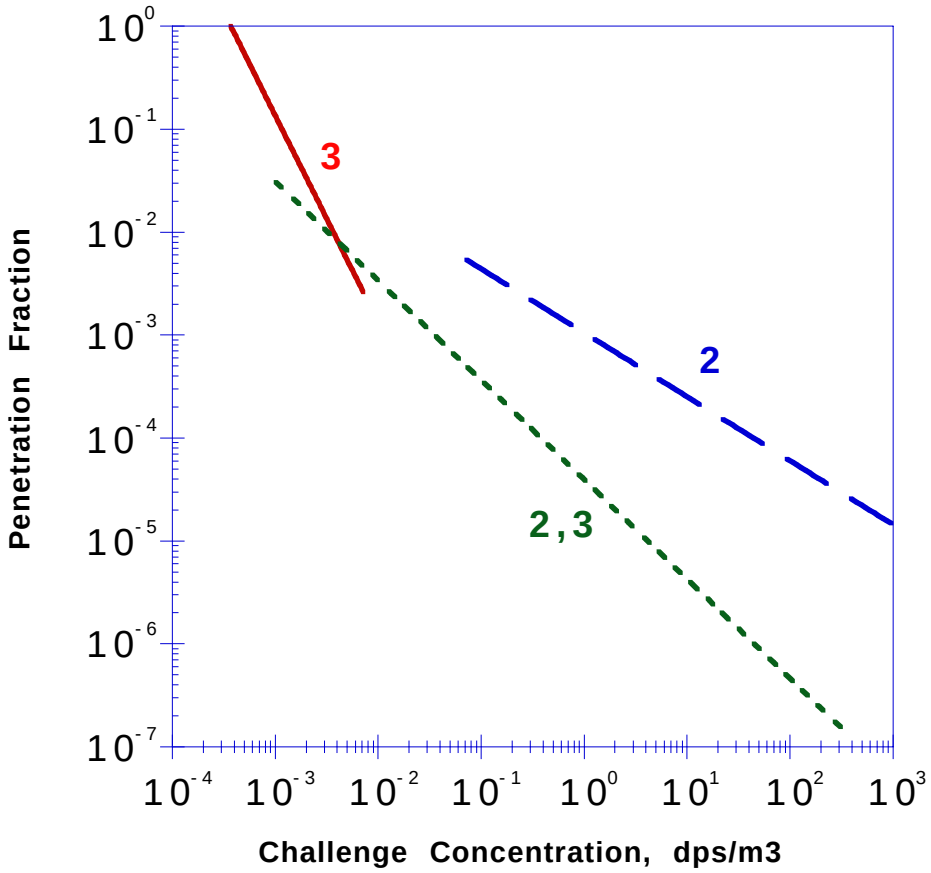

Figure 9. HEPA filter penetration fraction, P, as a function of Plutonium challenge concentration (Ci/m3) shows decreasing penetration with increasing concentration. The numbers next to the lines refer to the stage (2 or 3) or combined stages (2,3) of HEPA filtration. (Frigerio and Stowe 4)

We show in Figure 7 that the trend of higher efficiencies (or conversely lower penetrations) with increasing challenge concentration is consistent with the alpha recoil hypothesis. The trend in Figure 9 can also be used to support the alpha recoil hypothesis in absence of additional information. However, with the additional information that the observed higher penetrations are episodic and due to filter failures, moisture build-up, and accumulation of deposits on the downstream side of the HEPA filters, the trend in Figure 9 is therefore attributed to high background concentrations creating an artifact of lower filter penetration (higher filter efficiency) at increasing challenge concentration. In addition, the alpha recoil hypothesis predicts an increasing release of alpha emitting particles over time, whereas actual measurements show decreasing release following the episodic releases in Figure 8.

V DEVELOPMENT OF FILTRATION MEASUREMENT THEORY WITH TRANSIENT BACKGROUND

Two different sampling methods are used in determining the efficiency of HEPA filters: (A) extracting a sample of the air stream upstream and downstream of the HEPA filter and collecting the particulate sample on filters for analysis as shown in Figure 10, (B) collecting particulates on a HEPA filter and on one or more downstream HEPA filters and analyzing the HEPA filters or a portion of the HEPA filters as shown in Figure 11.

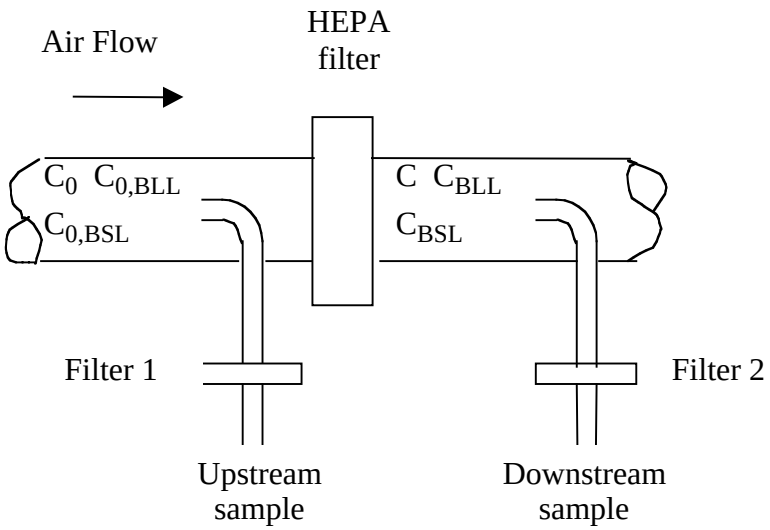

Figure 10. Schematic of filter efficiency measurement test using analysis of extract filter samples of the upstream and downstream concentrations.

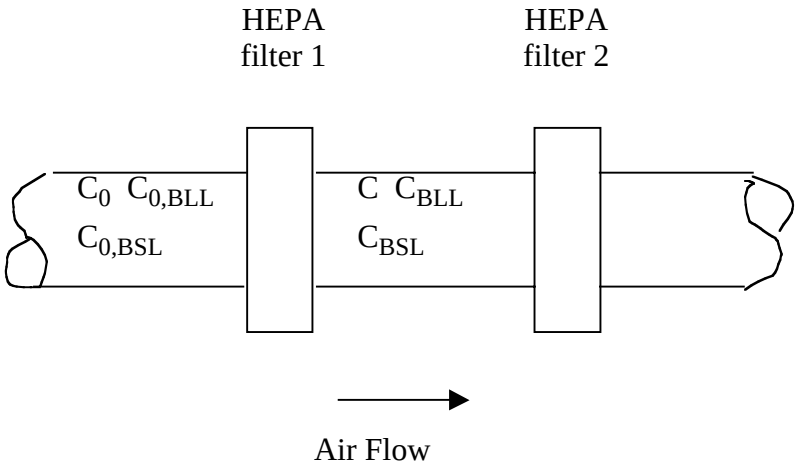

Figure 11. Schematic of filter efficiency measurement test using analysis on HEPA filters 1 and 2.

The two methods for determining HEPA filter efficiency as shown in Figures 10 and 11 are equivalent. The laboratory tests conducted by Ryan et al (1) and McDowell et al (2) are conducted using the system shown in Figure 11. Ryan et al (1) also use the system in Figure 11 for determining the efficiency of 1,000 cfm HEPA filters in field installations. They measure the radioactivity on small samples of the HEPA media and report the counts per minute per square inch of media. However, most field evaluations of HEPA filters use the extract system shown in Figure 10.

Both measurement methods rely on counting the radioactivity on two filter samples, one representing the challenge material collected on the upstream filter 1 and the other representing the material passing through the HEPA filter and collected on the downstream filter 2. In the configuration shown in Figure 11, the upstream filter 1 and downstream filter 2 are HEPA filters. The measured penetration is the ratio of the radioactive counts on the downstream filter 2 to the radioactive counts on the upstream filter 1. Since the number of counts will vary with the sample flow rate, the sample time, and the counting time, the measured counts must be divided by these variables to determine the penetration fraction from the two measurements.

$$P_M = \frac{R_2 / Q_2 t_{S2} t_{C2}}{R_1 / Q_1 t_{S1} t_{C1}} \qquad (5)$$

where P_M = Measured filter penetration
R_1 = Radioactive counts on Filter 1
R_2 = Radioactive counts on Filter 2
Q_1 = Flow rate through Filter 1
Q_2 = Flow rate through Filter 2
t_{s1} = Sample time through Filter 1
t_{s2} = Sample time through Filter 2
t_{c1} = Counting time for Filter 1
t_{c2} = Counting time for Filter 2

The radioactive species that produce the counts can be divided into long life species and short life species depending on their half life. For our purposes the short life species are the radon and thoron decay products. They have half lives ranging from minutes to hours. To simplify the derivation of the experimental penetration equation, we divide the total radioactivity on each filter into long life and short life components.

$$P_M = \frac{\left(R_{2,LL} + R_{2,SL}\right) / Q_2\, t_{S2}\, t_{C2}}{\left(R_{1,LL} + R_{1,SL}\right) / Q_1\, t_{S1}\, t_{C1}} \qquad (6)$$

where $R_{1,LL}$ = Radioactive counts on Filter 1 from the long life species
$R_{1,SL}$ = Radioactive counts on Filter 1 from the short life species
$R_{2,LL}$ = Radioactive counts on Filter 2 from the long life species
$R_{2,SL}$ = Radioactive counts on Filter 2 from the short life species

Transient behavior of short life species.

The background short life concentrations are primarily due to the radon and thoron daughters that have half lifes on the order of minutes and hours. Since plutonium and uranium processing facilities generally have significant quantities of radon and thoron daughters, they can affect the filter penetration measurements, especially for the higher filtration stages where the challenge concentration is extremely low. The background concentrations are a problem even at locations far removed from nuclear facilities. Radon is ubiquitous in the environment, so low concentration measurements will be in error if the background radon and its daughters is not accounted for. For example, Ryan et al (1) use background radioactive counts to measure a filter efficiency of 99.98% thereby implying background concentrations more than 10,000 times greater than their detection limits.

Because the radioactivity of the short life species (e.g. radon and thoron and their daughters) that are collected on a filter may change significantly in the two sequential processes of sampling followed by counting, we must include the time dependency in the short life species in Equation 6. We can derive the appropriate equation for the sampling process from the rate of the background accumulation in the filter and the rate of their decay. The derivation begins with the determination of the mass of the radioactive species trapped on the filter.

$$\frac{d\,M_{SL}}{d\,t_s} = C_{SL} Q - k\, M_{SL} \qquad (7)$$

where M_{SL} = Radioactive mass (counts/ sec) of short life background species trapped on filter
t_s = Sample time
C_{SL} = Concentration (counts/sec/m^3) of short life background species being filtered

Q = Flow rate, m^3/sec

k = $0.693/ t_{1/2}$ = Constant, sec^{-1}

$t_{1/2}$ = Half life, sec

The solution of Equation 7 is

$$M_{SL} = \frac{C_{SL} Q}{k}\left(1 - e^{-k t_s}\right) \qquad (8)$$

Equation 8 represents the radioactive mass (counts/sec) of the short life background species collected on the filter at the sampling time, t_s. This represents the mass at the sampling time, t_s. However, once the filter is removed from the collection system as shown in Figures 10 and 11, the radioactive mass (counts/sec) begins to reduce due to radioactive decay as shown in Equation 9.

$$M_{SL} = \frac{C_{SL} Q}{k}\left(1 - e^{-k t_s}\right) e^{-k t_D} \qquad (9)$$

where t_D = Delay time from the end of the sampling period, t_S, to the beginning of the measurement

When the filter is inserted into a counting apparatus such a scintillation counter or a proportional counter, the counter integrates counts while the radioactive mass continues to decay. Since the radioactive mass in Equation 9 represents a constant value, we have to add an additional decay time to represent the counting time. The resulting equation is then integrated over the counting time as shown in Equation 10.

$$R_{SL} = \int_0^{t_C} \frac{C_{SL} Q}{k}\left(1 - e^{-k t_s}\right) \varepsilon_{SL}\, e^{-k\left(t_D + t\right)}\, dt \qquad (10)$$

where t = Counting time, sec

ε_{SL} = Counting efficiency for particular method and short lived species.

The solution for Equation 10 is given by Equation 11.

$$R_{SL} = \underbrace{\frac{C_{SL}\,Q}{k}\left(1 - e^{-k\,t_S}\right)}_{\text{Sampling term}}\underbrace{e^{-k\,t_D}}_{\text{Delay term}}\underbrace{\frac{\varepsilon_{SL}}{k}\left(1 - e^{-k\,t_C}\right)}_{\text{Counting term}} \qquad (11)$$

Equation 11 shows that the radioactive counts for the short life species, R_{SL}, is the product of a sampling term, a delay term and a counting term. There are several limiting cases of interest in Equation 11.

For short sample, delay and counting times when $t_S << t_{1/2}$, $t_D << t_{1/2}$, and $t_C << t_{1/2}$,

$$R_{SL} \approx \varepsilon_{SL} C_{SL}\, Q\, t_S\, t_C \qquad (12)$$

For long delay times for any sample and counting times when $t_D >> t_{1/2}$ for any t_S and t_C,

$$R_{SL} \approx 0 \qquad (13)$$

For long sample times and any delay and counting times when $t_S >> t_{1/2}$ for any t_D and t_C .

$$R_{SL} \approx \frac{C_{SL}\,Q}{k}\, e^{-k\,t_D}\, \frac{\varepsilon_{SL}}{k}\left(1 - e^{-k\,t_C}\right) \qquad (14)$$

For long counting times and any delay and sampling times when $t_C >> t_{1/2}$ for any t_D and t_S .

$$R_{SL} \approx \frac{C_{SL}\,Q}{k}\left(1 - e^{-k\,t_S}\right) e^{-k\,t_D}\, \frac{\varepsilon_{SL}}{k} \qquad (15)$$

General Filter Penetration Equation:

To develop the general filter penetration equation, we need terms for both the short life species and the long life species. The comparable equation for the radioactive counts for the long life species, RLL, is given by,

$$R_{LL} = \varepsilon_{LL} C_{LL} Q t_S t_C \qquad (16)$$

The equations for the concentration C_{SL} in Equation 11 and C_{LL} in Equation 16 for filters 1 and 2 in terms of the concentrations shown in Figures 7 and 9 are given by .

$$C_{1,LL} = C_0 + C_{0,BLL} \qquad (17)$$

$$C_{1,SL} = C_{0,BSL} \qquad (18)$$

$$C_{2,LL} = (P_F + P_L)(C_0 + C_{0,BLL}) + C_{BLL} \qquad (19)$$

$$C_{2,SL} = (P_F + P_L) C_{0,BSL} + C_{BSL} \qquad (20)$$

$$C_P = P_F (C_0 + C_{0,BLL} + C_{0,BSL}) \qquad (21)$$

$$C_L = P_L (C_0 + C_{0,BLL} + C_{0,BSL}) \qquad (22)$$

where P_F = Filter penetration in absence of leaks or background interference

P_L = Filter leak

C_P = Concentration of species penetrating through the filter

C_L = Concentration of species leaking through or around the filter

Equations 11 and 16 are substituted into Equation 6 to yield the measured penetration

$$P_M = \frac{\left[\varepsilon_{LL} C_{2,LL} Q_2 t_{s2} t_{c2} + \frac{C_{2,SL} Q_2}{k}\left(1 - e^{-k t_{s2}}\right) e^{-k t_{D2}} \frac{\varepsilon_{SL}}{k}\left(1 - e^{-k t_{c2}}\right)\right] \Big/ Q_2 t_{s2} t_{c2}}{\left[\varepsilon_{LL} C_{1,LL} Q_1 t_{s1} t_{c1} + \frac{C_{1,SL} Q_1}{k}\left(1 - e^{-k t_{s1}}\right) e^{-k t_{D1}} \frac{\varepsilon_{SL}}{k}\left(1 - e^{-k t_{c1}}\right)\right] \Big/ Q_1 t_{s1} t_{c1}} \qquad (23)$$

where the concentration terms $C_{1,LL}$, $C_{1,SL}$, $C_{2,LL}$, and $C_{2,SL}$ are given by Equations 17-20 respectively.

Equation 23 represents the general equation for determining the filter penetration by radioactive counting of filter samples in the configurations shown in Figures 10 and 11 and in the presence of short and long life background radioactive species.

Although Equation 23 is a correct expression for the penetration measurement across the HEPA filter it includes much more complicated terms. For example, all of the concentration and filter penetration and leak terms in Equations 17- 23 are dependent on particle size. Moreover, the concentration of species penetrating the filter , C_P , will change with particle deposits (decrease with solid particles ; increase with liquid particles following an initial decrease) or with added moisture. In somewhat similar fashion, the concentration of species leaking through or around the HEPA filter, C_L, will vary with particle deposits. Moisture build-up in the HEPA filter will affect both species leaking and penetrating the HEPA filter. Increased filter penetration due to moisture or higher air flows also has a constant penetration independent of challenge . In addition, the various background concentrations are typically complex, time dependent functions with several terms. We will ignore all of the complications except for the specific parameters that affect the analysis of the hypothesized alpha recoil enhancement of HEPA filter penetration.

It is important to distinguish the difference between background concentration and leaks through or by-pass around the HEPA filter. The background concentration exists independent of the challenge concentration. There is a measurable background concentration even if the upstream HEPA filter concentration is 0. A leak or by-pass increases the measured concentration downstream of the HEPA filter in direct proportion to the challenge concentration as shown in Equation 22. Therefore, leaks have a constant penetration value, P_L , even with changing challenge concentration. The total penetration from the filter leaks is given by Equation 22

Typical causes of leaks are defective or improper gasket seals and defects or tears in the filter media. HEPA filter leak tests are required for all nuclear facilities after installation and every 18 months or sooner thereafter. Examples of potential sources for by-pass leaks include liquid drains, instrument ports, and electrical and water conduits . Care must be taken to ensure that all of the by-pass leaks are included in the leak tests.

Although all of the concentration and penetration terms in Equations 17-23 are time dependent, only the background short life concentrations are significant for most efficiency measurements. The changes to the filter and leak penetrations occur quite slowly and can be considered as constant during the efficiency measurements. Changes to the background concentrations of species with long life also occur over a much longer time period compared to the efficiency measurement and therefore can be considered

constant. For example Figerio and Stowe (4) find that plutonium holdup in ducts following episodic releases decays with a half life of three weeks to several months. This is a much longer time period than most filter efficiency measurements.

Although Equation 23 is rather unwieldy, it can be simplified for various limiting cases as described previously for the approximations given by Equations 12-15. We will consider the approximations in the following.

Approximation: $t_s << t_{1/2}$, $t_D << t_{1/2}$, and $t_C << t_{1/2}$

For short sample, delay and counting times compared to the half life of the species, Equation 23 reduces to

$$P_M = \frac{\varepsilon_{LL} C_{2,LL} + \varepsilon_{SL} C_{2,SL}}{\varepsilon_{LL} C_{1,LL} + \varepsilon_{SL} C_{1,SL}} \tag{24}$$

Assuming the counting efficiencies for the short life (ε_{SL}) and long life (ε_{LL}) species are the same, we have

$$P_M = \frac{C_{2,LL} + C_{2,SL}}{C_{1,LL} + C_{1,SL}} \tag{25}$$

Substituting Equations 17-20 and simplifying, we have

$$P_M = P_F + P_L + \frac{C_{BLL} + C_{BSL}}{C_0 + C_{0,BLL} + C_{0,BSL}} \tag{26}$$

where P_M = Measured filter fractional penetration
C_0 = Source challenge concentration
$C_{0,BLL}$ = Background long life challenge concentration
$C_{0,BSL}$ = Background short life challenge concentration
C_{BLL} = Background long life downstream concentration
C_{BSL} = Background short life downstream concentration

At high challenge concentrations, C_0 , Equation 26 shows the background becomes negligible leaving the fraction term approach zero and the measured penetration constant as a function of challenge concentration.

$$P_M \approx P_F + P_L \tag{27}$$

At lower concentrations, the downstream background concentrations (C_{BLL} and C_{BSL}) become significant and the penetrations P_F and P_L negligible compared to the quotient. Under these conditions Equation 26 reduces to

$$P_M \approx \frac{C_{BLL} + C_{BSL}}{C_0} \tag{28}$$

Under these conditions, Equation 28 shows the measured penetration decreases inversely with increasing challenge concentration.

When the challenge concentration becomes negligibly small (as may occur after multiple HEPA filters in series) Equation 26 becomes dominated by the background terms and yields Equation 29.

$$P_M \approx \frac{C_{BLL} + C_{BSL}}{C_{0,BLL} + C_{0,BSL}} \tag{29}$$

Note that under background domination, the measured penetration is not only very high, but it is also independent of the challenge concentration, C_0 .

Thus, depending on the magnitude of the challenge concentration, the measured penetration can go from Equation 27 at very high concentrations, to Equation 28 at intermediate concentrations, and finally to Equation 29 at very low concentrations.

Approximation: $t_D >> t_{1/2}$ for any t_S and t_C,

For the approximation where the filter samples have a long delay after sampling and prior to counting in order to remove the short life species, Equation 23 becomes

$$P_M = \frac{C_{2,LL}}{C_{1,LL}} \tag{30}$$

Substituting the values for $C_{1,LL}$ and $C_{2,LL}$ from Equations 17 and 19 respectively, into Equation 30, we have after simplifying,

$$P_M = P_F + P_L + \frac{C_{BLL}}{C_0 + C_{0,BLL}} \tag{31}$$

Note that Equation 31 is similar to Equation 26 where all the experimental times ($t_s << t_{1/2}$, $t_D << t_{1/2}$, and $t_C << t_{1/2}$) are short compared to the half life. However Equation 31 has no short life species as expected from the approximation of a long time delay to allow all the short life species to decay.

A series of approximations of Equation 31 can be made depending on the challenge concentration, C_0, similar to the previous approximations made in Equations 27-29.

At high challenge concentrations, C_0 , Equation 31 shows the background becomes negligible leaving the fraction term approach zero and the measured penetration constant as a function of challenge concentration.

$$P_M \approx P_F + P_L \tag{32}$$

At high challenge concentrations, the measured penetration is independent of the challenge concentration and equals the sum of the filter penetration plus leak.

At lower concentrations, the downstream background concentrations (C_{BLL}) become significant and the penetrations P_F and P_L negligible compared to the quotient. Under these conditions Equation 31 is reduced to

$$P_M \approx \frac{C_{BLL}}{C_0} \tag{33}$$

Under these conditions, Equation 33 shows the measured penetration decreases inversely with increasing challenge concentration.

When the challenge concentration becomes negligibly small (as may occur after multiple HEPA filters in series) Equation 31 becomes dominated by the background terms and yields Equation 34.

$$P_M \approx \frac{C_{BLL}}{C_{0,BLL}} \tag{34}$$

Note that under background domination, the measured penetration is not only very high, but it is also independent of the challenge concentration, C_0 .

Thus, depending on the magnitude of the challenge concentration, the measured penetration can go from Equation 32 at very high concentrations, to Equation 33 at intermediate concentrations, and finally to Equation 34 at very low concentrations.

Approximation: $t_S >> t_{1/2}$ for any t_D and t_C

For very long sampling times, Equation 23 is reduced to

$$P_M = \frac{\varepsilon_{LL} C_{2,LL} + \frac{C_{2,SL}}{kt_{S2}}\, e^{-k t_{D2}}\, \frac{\varepsilon_{SL}}{kt_{C2}}\left(1 - e^{-k t_{C2}}\right)}{\varepsilon_{LL} C_{1,LL} + \frac{C_{1,SL}}{kt_{S1}}\, e^{-k t_{D1}}\, \frac{\varepsilon_{SL}}{kt_{C1}}\left(1 - e^{-k t_{C1}}\right)} \tag{35}$$

Equation 23 is further simplified for long sample times (very large t_S) by making the exponential terms negligible and yields,

$$P_M \approx \frac{C_{2,LL}}{C_{1,LL}} \tag{36}$$

Note that Equation 36 for the long sample time approximation is identical to Equation 30 for the long delay time. As a result the corresponding penetration and the dependencies on challenge concentration will also be identical.

However, a much longer sample time is required to yield the same approximation (Equation 36) as for an equivalent delay time (t_D) (Equation 30). This follows because the sample time reduces the interfering short life counts in a linear fashion (see Equation 35) whereas the delay time reduces the interfering species in an exponential fashion (see Equation 23). Moreover, the delay time eliminates the short life counts directly, whereas the increased sampling time effectively dilutes the short life counts with increased long life counts from the long sample.

Substituting the values for $C_{1,LL}$ and $C_{2,LL}$ from Equations 17 and 19 respectively, into Equation 36, we have after simplifying,

$$P_M = P_F + P_L + \frac{C_{BLL}}{C_0 + C_{0,BLL}} \qquad (37)$$

Note that Equation 37 is identical to Equation 31 where $t_D << t_{1/2}$ and is similar to Equation 26 where all the experimental times ($t_S << t_{1/2}$, $t_D << t_{1/2}$, and $t_C << t_{1/2}$) are short compared to the half life.

A series of approximations of Equation 37 can be made depending on the challenge concentration, C_0, similar to the previous approximations made in Equations 27-29 for short experimental times and in Equations 32-34 for long delay times.

At high challenge concentrations, C_0 , Equation 37 shows the background becomes negligible leaving the fraction term approach zero and the measured penetration constant as a function of challenge concentration.

$$P_M \approx P_F + P_L \qquad (38)$$

At high challenge concentrations, the measured penetration is independent of the challenge concentration and equals the sum of the filter penetration plus leak.

At lower concentrations, the downstream background concentrations (C_{BLL}) become significant and the penetrations P_F and P_L negligible compared to the quotient. Under these conditions Equation 37 is reduced to

$$P_M \approx \frac{C_{BLL}}{C_0} \tag{39}$$

Under these conditions, Equation 39 shows the measured penetration decreases inversely with increasing challenge concentration.

When the challenge concentration becomes negligibly small (as may occur after multiple HEPA filters in series) Equation 37 becomes dominated by the background terms and yields Equation 40.

$$P_M \approx \frac{C_{BLL}}{C_{0,BLL}} \tag{40}$$

Note that under background domination, the measured penetration is not only very high, but it is also independent of the challenge concentration, C_0 .

Thus, depending on the magnitude of the challenge concentration, the measured penetration can go from Equation 38 at very high concentrations, to Equation 39 at intermediate concentrations, and finally to Equation 40 at very low concentrations.

Approximation: large t_C .

For the approximation of very long counts, Equation 23 is reduced to

$$P_M = \frac{\varepsilon_{LL} C_{2,LL} + \frac{C_{2,SL}}{kt_{S2}}\left(1 - e^{-k t_{S2}}\right) e^{-k t_{D2}} \frac{\varepsilon_{SL}}{kt_{C2}}}{\varepsilon_{LL} C_{1,LL} + \frac{C_{1,SL}}{kt_{S1}}\left(1 - e^{-k t_{S1}}\right) e^{-k t_{D1}} \frac{\varepsilon_{SL}}{kt_{C1}}} \tag{41}$$

Note that Equation 41 for the long counting time is similar to Equation 35 for the long sampling time. Because of this similarity, the resulting approximations given by Equations 38-40 for the long sampling will approach the same equation for the long

counting. This follows since Equation 41 reduces to Equation 42 at long $\mathbf{t_C}$ which is identical to Equation 36 for long sampling time.

$$P_M \approx \frac{C_{\mathbf{2,LL}}}{C_{\mathbf{1,LL}}} \qquad (42)$$

Therefore, the approximations for the penetration at different challenge concentrations given by Equations 38-40 apply to the long counting condition.

General approximation for all experimental test conditions

Based on the four cases analyzed, we can state that the measured penetration in the presence of background interference will show the same trend with respect to the challenge concentration independent of the sampling times, delay times and counting times. The general equation for the measured filter penetration for all test conditions is

$$P_M = P_F + P_L + \frac{C_B}{C_0 + C_{0,B}} \qquad (43)$$

where C_B = Downstream background concentration of short and/or long life species

$C_{0,B}$ = Challenge background concentration of short and/or long life species

At high challenge concentrations the penetration is independent of challenge concentration:

$$P_M \approx P_F + P_L \qquad (44)$$

At intermediate challenge concentrations the penetration is inversely dependent on the challenge concentration:

$$P_M \approx \frac{C_B}{C_0} \qquad (45)$$

At very low challenge concentrations, the penetration is once again independent of the challenge concentration:

$$P_M \approx \frac{C_B}{C_{0,B}} \qquad (46)$$

Since the background concentrations are typically of the same order of magnitude before and after the HEPA filter, with $C_{0,B} > C_B$, the measured penetration from Equation 46 is usually quite high.

VI FILTER EFFICIENCY MEASUREMENT THEORY IS IN AGREEMENT WITH EXPERIMENTAL DATA

Frigerio and Stowe Study

We compare the experimental results of field and laboratory tests to the theory of filter measurement in the presence of background interference and find good agreement. The field measurements of filter penetration, P_M, from Frigerio and Stowe (4) in Figure 9 are compared to theoretical computations using Equation 43 for various fixed values of background concentration, C_B, and challenge background concentration, $C_{0,B}$, in Figure 12. The range of the challenge concentration, C_0 , is chosen to include the data from Frigerio and Stowe (4) in Figure 9 for the second and third stage HEPA filters and the estimate by Gonzales et al (13) for the maximum challenge concentration of 3.7×10^5 dps/m^3 (10^{-5} μCi/ml) expected in a nuclear facility. We use the value 2×10^{-5} from Frigerio and Stowe (4) for the penetration ($P_F + P_L$) (99.998% efficiency) of a single stage HEPA filter. The background concentrations, C_B, are arbitrarily selected to cover the range of the experimental penetration versus C_0 curves for HEPA filter stages two and three in Figure 9.

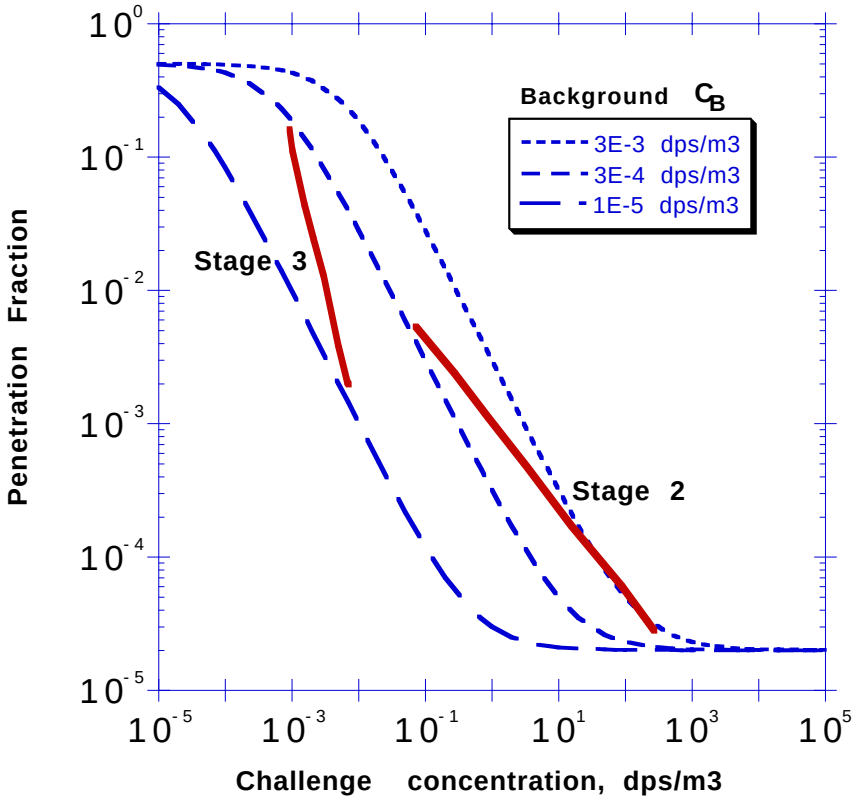

Figure 12. Comparison of theoretical filter penetration from Equation 43 (dashed lines) for various background concentrations plotted as a function of the challenge concentration. The solid lines are the experimental data for HEPA filter stages 2 and 3 from Figure 9. The HEPA filter for stage 1 has an experimental penetration of 0.00002 (99.998%), but no data is presented as a function of upstream concentration (Frigerio and Stowe 4)

The parameters used in Equation 43 to generate the theoretical curves in Figure 12 are tabulated in Table 3.

Table 3. Parameters used in Equation 43 to compute penetration curves in Figure 12

Study	$P_F + P_L$	$C_{0,B}$	C_B
Frigerio (4)	2E-5	6E-3	3E-3
Frigerio (4)	2E-5	6E-4	3E-4
Frigerio (4)	2E-5	2E-5	1E-5

The primary features of the computed HEPA filter penetration curves in Figure 12 are the increasing filter penetration at lower challenge concentrations due to the background concentration and the convergence to a constant filter penetration at higher challenge concentrations. The curves are derived from Equation 43 and illustrate the

approximation of Equation 44 for filter dominated penetration at high concentrations and Equation 46 for background dominated penetration at low concentrations. At intermediate challenge concentrations, the penetration equals the background concentration divided by the challenge concentration as given in Equation 45. Note that the transition from the filter dominated to the background dominated condition occurs at higher challenge concentrations with increasing background concentrations. Also note that in the region dominated by background concentration, the measured penetration is independent of the challenge concentration as required from Equation 46.

In general the experimental curves are consistent with the theoretical predictions. The second stage HEPA filter falls between the background concentration of $3x10^{-4}$ dps/m^3. and $3x10^{-3}$ dps/m^3 .The third stage HEPA filter falls between the background concentrations of $1x10^{-5}$ and $3x10^{-4}$ dps/m^3. These trends are consistent with experimental observations where the background concentrations after the third stage HEPA filters are significantly less than the corresponding background concentrations after the second stage HEPA filter. At much higher values of C_0 , as would occur for the first stage HEPA filter, there is little or no dependence of the measured filter penetration on C_0 . However, Frigerio and Stowe do not provide any data for the first stage HEPA filter as a function of the challenge concentration.

A quantitative comparison between the experimental HEPA penetration curves obtained by Frigerio and Stowe (4) and the theoretical curves generated with Equation 43 show some discrepancies. The equation for the experimental curve in Figure 12 for the third stage filter is $P_M = 10^{-6.8795}/C_0^{2.005}$, which shows a higher exponent for the concentration dependency than that given by Equations 43 or 45 . The equation for the second stage HEPA filter is $P_M = 10^{-2.9778}/C_C^{0.62154}$, which shows a reduced dependency on C_0.as expected from theory whereby the dependency on challenge concentration decreases with increasing challenge concentration. The equation for the combined filter stages 2 and 3 is $P_M = 10^{-4.4033}/C_0^{0.96607}$, which is intermediate between that for the separate stage 3 and stage 2.

Equations 43 and 45 show the maximum power of the challenge concentration cannot exceed one while the experimental data for the stage three HEPA filter is 2.005. This discrepancy is due to the method in which Frigerio and Stowe obtained the data. The experimental curves from Figure 9 are generated by measuring the transient concentrations in Figure 8 at weekly and sometimes daily intervals for each of the two HEPA filter stages in order to obtain the large range in challenge concentrations. Frigerio and Stowe note that the transient measurements of the exhaust from the third stage HEPA filter show a slow decreases in concentration following the release episodes with the resulting increase in the challenge concentration. The slow releases are attributed to deposits in the ducting that are formed during the release episodes. Frigerio and Stowe use gamma ray measurements along the duct to verify the deposits. Following the

episodic releases, the transient challenge concentration quickly decreases while deposits downstream of the filter become re-suspended and increase the background concentration in a transient fashion until the deposits are removed.

These transient deposits and releases of the background concentrations, C_B, are responsible for the apparent disagreement between the experimental measurements and theory. The computed theoretical curves in Figure 12 are generated assuming a constant background concentration. However, if we allow the background concentration to vary as occurrs with the episodic releases from Figure 8, then the theory agrees with the experiment.

Orth et al (14) study on the efficiency of a deep bed sand filter

Orth et al measure the efficiency of a deep bed sand filter over several years and find the efficiency increases with increasing challenge concentration (14). Figure 13 shows the fractional penetration (1 - fractional efficiency) decreases with increasing challenge concentration. The data also shows that the penetration decreases from the period 4/76-12/78 to 1/79-6/80. Orth attributes the decreased penetration to the increase in particle deposits, which results in lower penetration. Separate curves are drawn through the two data sets using a least squares fit to Equation 43. The penetration measurements are obtained from alpha radiation measurements before and after the sand filter. No discussion is made regarding the removal of short life species that may dominate the downstream measurement in deep bed sand filters as Zippler (15) reports and is presented later in this paper. The variability in the radiation measurements over time provides the range in challenge concentration and penetration data shown in Figure 13.

Orth et al states that the concentration dependence on the penetration is due to the release of a small amount of previously deposited particles (14). The attrition of particle deposits from a packed granular bed is a well known phenomenon. These deposits would contribute to the release of long life species. In addition, there are short life species from gaseous radon and thoron as reported by Zippler that are also released (15). We assume the data from Orth represents the long life species after subtracting the short life species.

We also fit the data in Figure 13 to Equation 45 and find $P_M = 0.0878/C_0^{1.19}$ and $P_M = 0.0496/C_0^{1.17}$ for the 4/76-12/78 and the 1/79-6/80 data sets. These curves are not shown in Figure 13. The fact the challenge concentration has an exponent around one indicates that the background concentration is sufficiently high and the challenge sufficiently low to have the penetration in the transition region between filter dominated and background dominated regions. Since the exponent for the challenge concentration is slightly greater than one, it suggests a transient build up and release of deposits as observed by Frigerio and Stowe for the HEPA filter studies. This suggestion is reasonable since the measurements are taken over time and include transients of higher emissions.

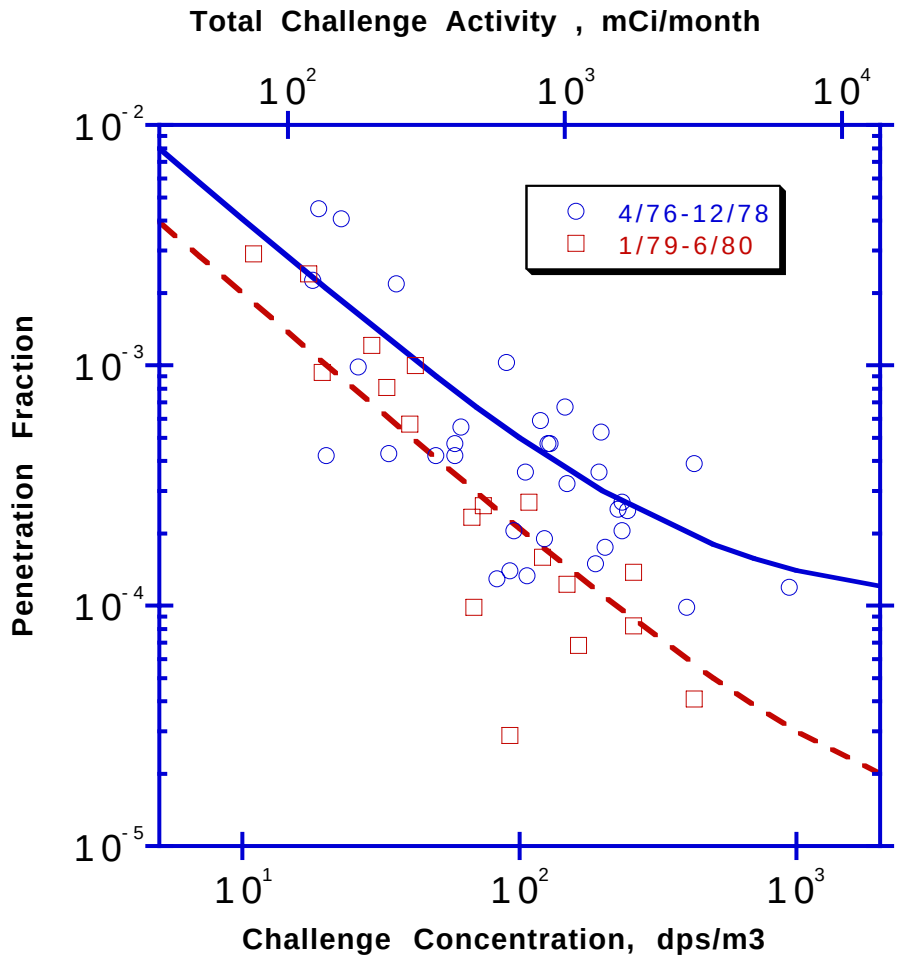

Figure 13 Fractional penetration through sand filter as a function of upstream alpha activity concentration Activity concentration in dps/m^3 is computed from mCi/mo assuming 205,000 cfm through the sand filter. The curves represent theoretical penetration with a background concentration computed from Equation 43. (14)

We extrapolate the curves from Figure 13 to smaller and larger challenge concentrations in Figure 14 to show the full penetration curve with the limits at filter dominated and background dominated regions. The parameters used to generate the curves in Figures 13 and 14 are shown in Table 4.

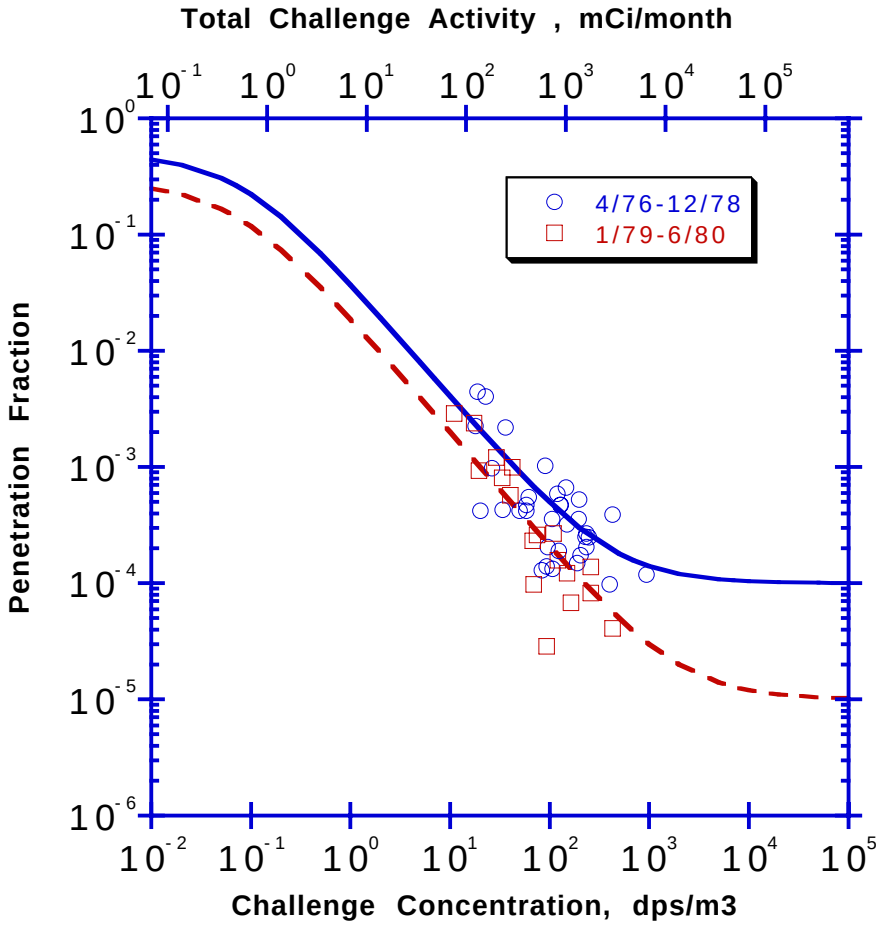

Figure 14 Fractional penetration through sand filter as a function of upstream alpha activity concentration Expanded graph from Figure 13 to show the complete theoretical penetration curve.

Table 4 . Parameters used in computed penetration curves for sand filter in Figures 13 and 14

Filter Test	$P_F + P_L$	$C_{0,B}$ (dps/m3)	C_B (dps/m3)
4/76-12/78	0.0001	0.08	0.04
1/79-6/80	0.00001	0.07	0.02

Ryan et al (1) and McDowell et al (2) studies on alpha recoil

We replot the data from the McDowell et al (2) and the Ryan et al (1) studies shown in Figures 6 and 7 and fit them to Equation 43 to demonstrate that the low HEPA filter efficiencies attributed to alpha recoil are better explained by background interference.

Figure 15 shows the penetration of 238Pu and 239Pu through HEPA filters as a function of the challenge concentration for the Ryan et al (1) and Hetland et al (3) field studies and for the McDowell et al (2) laboratory studies. The wide variety of data show excellent agreement with the filter background theory. There are a few additional observations that should be noted in Figure 15. The first stage HEPA filters in the Ryan1 field study have much lower penetrations than the filters in the Ryan2 field study because they presumably become clogged with deposits due to their longer life at 35 months compared to 27 months for the Ryan2 field study. Deposits of solid particles greatly reduce the filter penetration. Another observation is the identical penetrations for the two high concentration data points for the Hetland field study. These points represent the first and second stage HEPA filters. We arbitrarily set their penetration equal since the combined penetration is 10^{-5} and no guidance is given on their separate penetrations. The parameters used to generate the curves are shown in Table 5.

Table 5. Parameters used in computed penetration curves in Figure 15

Study	$P_F + P_L$	$C_{0,B}$	C_B
Hetland (3)	.00316	0.002	0.0014
Ryan2 (1)	2.39E-5	1.14E-6	3.37E-7
Ryan1 (1)	1.31E-6	8.98E-6	5.59E-6
McDowell (2)	0.0002	0.025	0.02

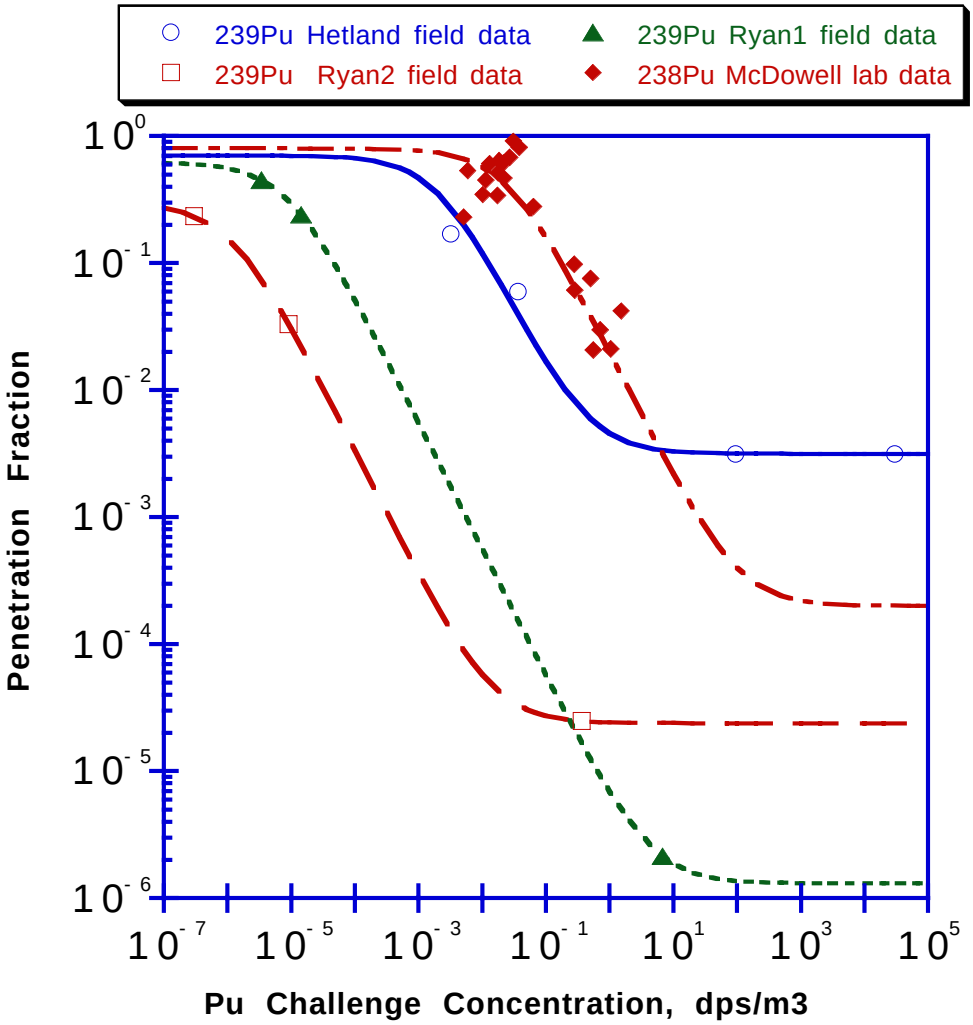

Figure 15. Filter penetration as a function of the challenge concentration for each filter stage of a multistage filter test system for 238Pu and 239Pu replotted from Figures 6 and 7 (1-3)

We replot the data from McDowell et al (2) for 212Pb penetration in Figure 16 and for 235Es penetration in Figure 17 using Equation 43. The parameter values for the curves in Figures 16 and 17 are given in Tables 6 and 7 respectively. Figure 16 shows that most of the data for the 212Pb penetration falls in the background dominated region except for two stage 1 HEPA filters that are in the transition region. Figure 17 shows that stage 2 and 3 HEPA filters are dominated by the background region, whereas all of the stage 1 HEPA filters are in the transition region

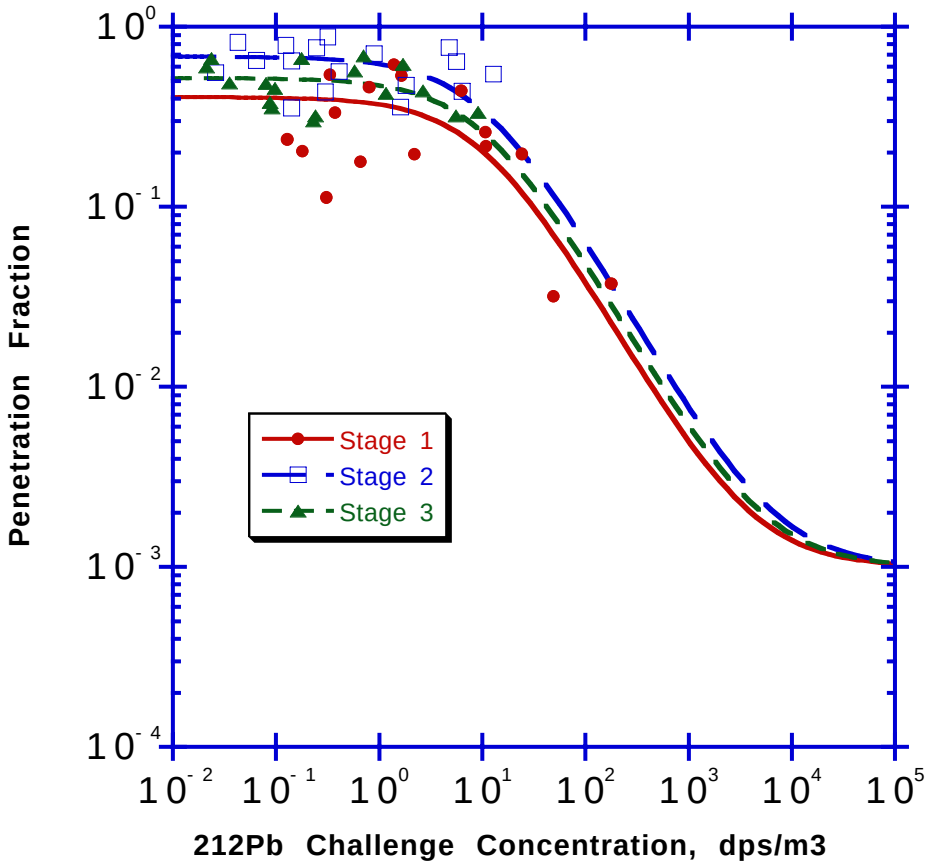

Figure 16. 212Pb filter penetration fraction as a function of challenge activity for first, second and third stages from McDowell et al (2).

Table 6 . Parameters used in computed penetration curves in Figure 16

Filter Stage	$P_F + P_L$	$C_{0,B}$ (dps/m3)	C_B (dps/m3)
1	0.0002	8	3
2	0.0002	4	2.7
3	0.0002	4	2

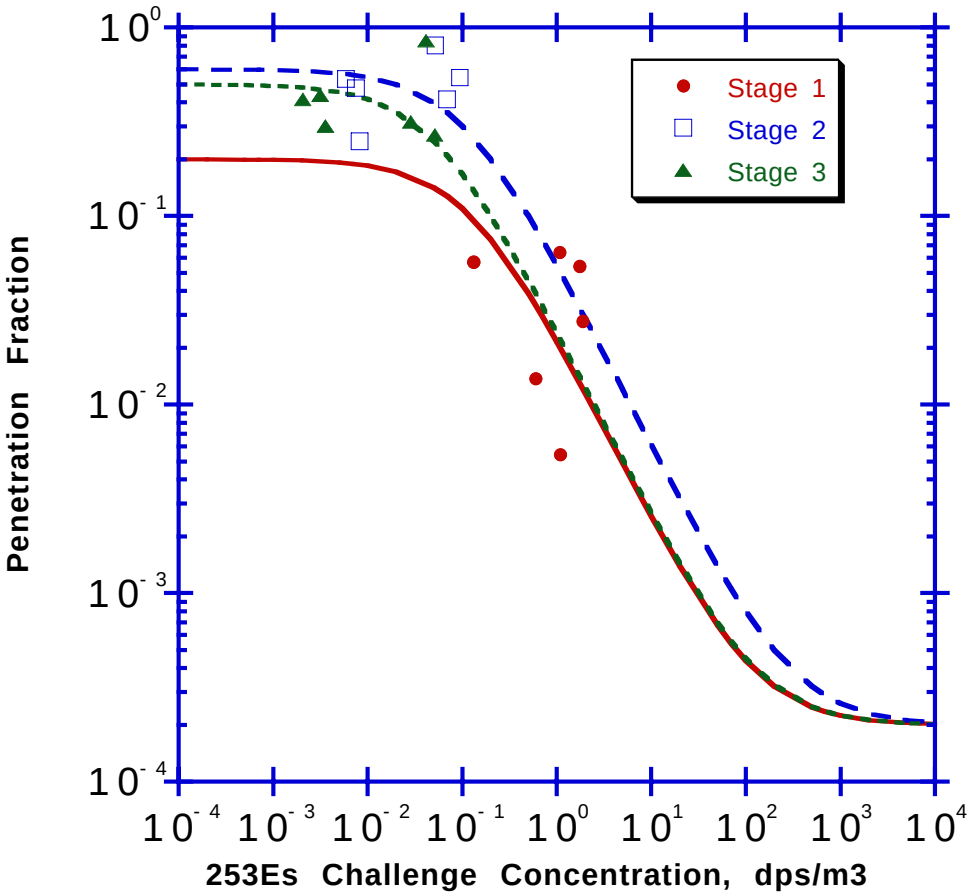

Figure 17. 253Es filter penetration as a function of challenge concentration for first, second and third stages from McDowell (2).

Table 7. Parameters used in computed penetration curves in Figure 17

Filter Stage	$P_F + P_L$	$C_{0,B}$ (dps/m3)	C_B (dps/m3)
1	0.0002	0.12	0.024
2	0.0002	0.10	0.06
3	0.0002	0.05	0.025

For completeness, we graph the initial data from Ryan et al (1) in Table 1 that is used to propose the hypothesis that alpha recoil nuclei can produce particle fragments and result in increased filter penetration. Figure 18 shows the data plotted as a least squares best fit to Equation 43. The numbers next to the data points represent the filter stage. The data and curve is in general agreement with the more extensive results shown in Figure 16.

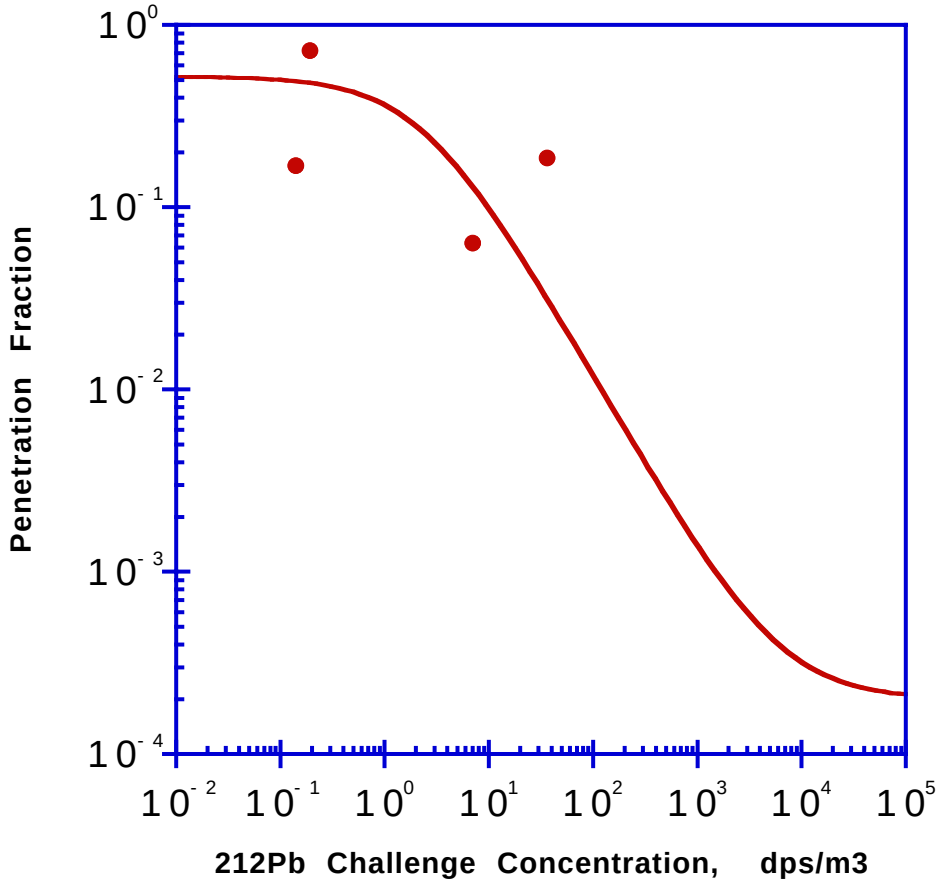

Figure 18. 212Pb filter penetration fraction as a function of challenge activity for four filter stages plotted with data from Table 1 with volume 1.8 m^3 (1). Parameter values used to generate the curve from Equation 40 are Pf + PL = 0.0002 , C_B = 1.2 dps/m^3. $C_{0,B}$ = 2.3 dps/m^3.

The reasonable fit of the test results from Ryan et al (1) and McDowell et al (2) shown in Figures 15-18 to Equation 43 suggests that the interference from the background concentration is a good explanation for the observed high filter penetration (low efficiency). However, in absence of additional measurements to independently confirm the background concentration, the reasonable fit to Equation 43 is not conclusive proof that background interference rather than alpha recoil is responsible for the high filter penetration.

VII SOURCES OF BACKGROUND INTERFERENCE AND MITIGATION TECHNIQUES

The primary sources for the background interference in HEPA filters are deposits in the exhaust system and from gaseous contaminants of radon and thoron. Leaks, by-pass and increased penetration due to water clogging in the HEPA filter or high air flows are not directly part of the background. However, they contribute to the background source by forming particle deposits that accumulate in ducts during periods of high concentration as noted by Fierro and Stowe (4) . Filter by-pass may also occur when replacing a filter during normal maintenance. A small amount of plutonium may spill on the clean side of the filter housing during filter change-out. When the new filter is installed and the air flow re-activated, any deposits on the clean side of the ducting and filter housings can be resuspended due to air turbulence and mechanical vibrations and then will be transmitted to the downstream HEPA filter. These previous deposits on the clean side of the filter can significantly reduce the measured HEPA filter efficiency.

Although there are no studies that specifically addressed how filter change-out and filter failures impact the observed filter efficiency, these factors unquestionably reduce the efficiency from what is measured under controlled conditions. Carbaugh identifies gasket, frame and media failures as causes for decreased filter efficiency (10). Fortunately, these failures are easily detected through the annual in-place efficiency tests. Most non-reactor facilities follow the guidance of Elder et al and use 99.9% efficiency for the first filter and 99.8% for the second and subsequent filters under accident conditions in which the filter is not structurally damaged (5) The lower efficiency is assigned to account for degraded performance under accident conditions rather than the lower HEPA filter efficiency observed in field studies. The study by Hettfield and Russell reports that the third stage HEPA filter only has an efficiency of 85% (3). They suspect that the most likely cause for the lower HEPA filter efficiencies is leakage around the HEPA filter. However, this is unlikely because in-place leak tests can readily detect the leak. Considering that Hettfield and Russell base their efficiency calculation on radiation measurements, a more probable cause is background measurements from deposit releases or gas contaminants .

Another major source of background for radiation measurements are the radon-thoron daughters that are ubiquitous in the environment, and especially around Pu and U sources. These sources are especially difficult to remove because radon is a gas that can penetrate and adsorb on all filters. The background radon and thoron concentrations can be much greater than the challenge concentrations from nuclear facilities, thereby making efficiency measurements difficult. Figure 19 illustrates the magnitude of the background thoron on the measured HEPA filter penetration in a study by Zippler (15). He installs a HEPA filter in the exhaust from a deep-bed sand filter to determine the additional reduction in emissions from a final stage HEPA filter after the sand filter (15.) Zippler collects filter samples before and after the HEPA filter at 3 cfm for 72-240 hours in order to obtain a sufficient sample. He then measures the activity of filter samples as a function of measurement time as seen in Figure 19. The decreasing activity with time is

due to the decay of short lived decay products. Zippler concludes the decay is due to thoron daughters.

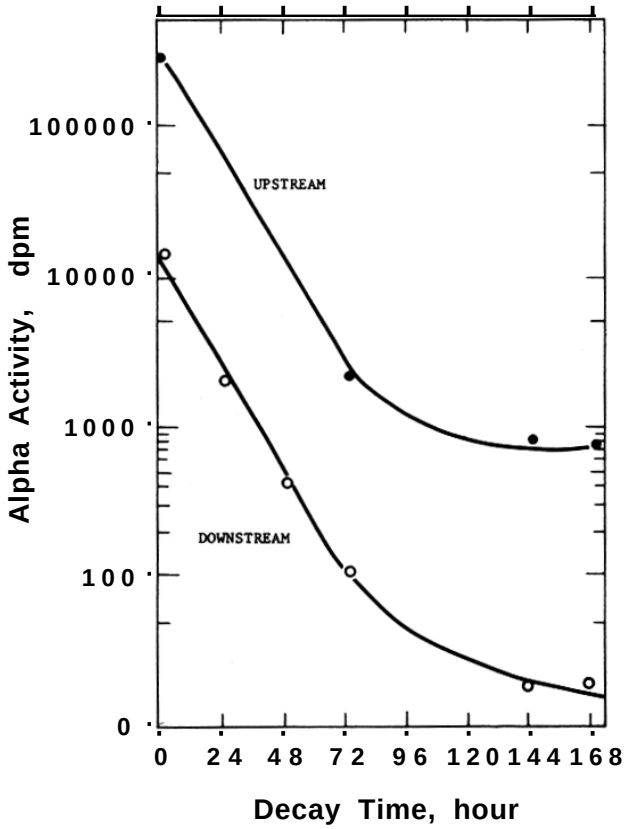

Figure 19. Measured alpha counts on filter samples taken before and after an additional HEPA filter (see Figure 10) installed in a 1,000 cfm slip stream in the exhaust from a deep bed sand filter at the Savannah River Plant. The filter samples are taken at 3 cfm for 144 hours and show the very large background radiation present in the air samples used to measure filter efficiency. (Zippler, 15)

The effect of the background concentration on the measured HEPA filter efficiency is most pronounced with the second and higher stages of HEPA filtration. This follows because the challenge concentration is greatly reduced with each stage of filtration, thereby making the background concentration more significant compared to the downstream concentration. The increased impact of the background concentration on the higher stages of HEPA filtration is seen in Figures 12- 18 and Equation 43 where the background concentration becomes increasingly more important as the challenge

concentration decreases. At very low challenge concentrations the penetration is dominated by the background concentration according to Equation 46.

For deep-bed sand filters an additional source of background concentration is due to the gradual release of previously deposited particles due to attrition of sand particles in the bed plus the release of short life species from gaseous radon and thoron . There is no comparable attrition loss in HEPA filters because the particle deposits are firmly held on the upstream side of the HEPA filter, and the filter media is not loose like the sand filter.

There are four approaches for reducing the impact of the background concentration (both short life and long life species) on the measured HEPA filter efficiency: (A) increase the challenge concentration, (B) increase the sampling time, (C) increase the delay time prior to counting to allow short life species to decay, and (D) increase the counting time. We can see this by analyzing the total counts, N_2, that represents the downstream filter sample in Equation 47.

(47)

$$N_2 = \varepsilon_{LL} C_{2,LL} Q_2 t_{s2} t_{c2} + \frac{C_{2,SL} Q_2}{k}\left(1 - e^{-k t_{s2}}\right) e^{-k t_{D2}} \frac{\varepsilon_{SL}}{k}\left(1 - e^{-k t_{c2}}\right)$$

At short counting (t_{C2}) and sampling (t_{S2}) times, Equation 47 becomes

$$N_2 = \varepsilon_{LL} C_{2,LL} Q_2 t_{s2} t_{c2} + C_{2,SL} Q_2 t_{s2} \left(e^{-k t_{D2}}\right) \varepsilon_{SL} t_{c2} \quad (48)$$

At long counting (t_{C2}) and sampling (t_{S2}) times, Equation 47 becomes

$$N_2 = \varepsilon_{LL} C_{2,LL} Q_2 t_{s2} t_{c2} + \frac{C_{2,SL} Q_2}{k}\left(e^{-k t_{D2}}\right) \frac{\varepsilon_{SL}}{k} \quad (49)$$

We see from Equations 48 and 49 that the concentration, counting time and sampling time increase the total counts in a linear fashion, whereas the delay time, t_D, reduces the short life species in an exponential fashion. The exponential decay of the short life species is the most effective means for mitigating this artifact from the background in the efficiency measurement. From Equation 49, we see that longer sampling times and longer counting times reduce the contribution from short life background species, $C_{2,SL}$,

but not from the long life species, $C_{2,LL}$. The short life species are typically radon and thoron decay products. For long life background species, e.g. resuspensions from wall deposits, increased sampling and counting times will not improve the efficiency measurement. However, if it is possible to increase the challenge concentration, then the background artifacts from long life species will be reduced as given by Equation 43. Thus, to mitigate the artifacts created from long life and short life background species, it is necessary to have long sampling times, long delay times, long counting times, and high challenge concentrations.

We suspect that the failure to follow these guidelines is responsible for the high filter penetrations observed by McDowell et al(2) and Ryan et al (1) as seen in Figures 15-18. It is also noteworthy that they do not discuss the background gaseous contaminants from radon and thoron daughters. In fact, the 212Pb source used in their studies is from the decay of thoron (1,2).

VIII EXPERIMENTS SHOW BACKGROUND INTERFERENCE IS RESPONSIBLE FOR THE MEASURED LOW HEPA FILTER EFFICIENCY

Gozales et al (13) conduct the definitive experiment demonstrating the efficiency of multi-stage HEPA filters against plutonium aerosols. The results refute the hypothesis proposed by Ryan et al (1) and McDowell et al (2) that plutonium fragments from alpha recoil lowers the HEPA filter efficiency. Even more convincing is that Gonzales et al conduct their experiments with well characterized 238Pu aerosols of comparable size to that measured in plutonium facilities and also used standard HEPA filters. Ryan et al (1) and McDowell et al (2) conduct their tests on 1.5 cm diameter filter media and do not use aerosols.

The study by Gonzales et al (13) demonstrates the filter measurement concepts in the previous section for filter efficiency measurements in the presence of interfering background. They show that high filter penetrations (low efficiencies) are obtained unless the samples used to compute the HEPA filter efficiency are obtained with long sample times, long counting times, long delay times and with very high challenge concentration. When these steps are taken, then the artifacts (i.e. low efficiency) disappear.

Gonzales et al (13) conduct a study of the filtration efficiency for each of three HEPA filters in series using $^{238}PuO_2$ aerosols under controlled laboratory conditions. They measure the radioactivity level of the Pu aerosols before and after each filter for 3 HEPA filters in 32 separate tests. The filters have the encapsulated design with 2 inch diameter inlet and exhaust ports and have a capacity of 25 cfm This type of filter eliminates the potential for gasket leaks that may occur with the standard open face filters widely used

in nuclear facilities. Otherwise, the design and materials of the filter pack is similar to the standard HEPA filter. Membrane filter samples are taken before and after each HEPA filter and counted. Because of the extremely low particle concentration after the third stage HEPA filter, Gonzales et al sample the entire 25 cfm using 9 separate filter disks to increase the amount of collected particles.

In their initial tests, Gonzales et al find contamination at the third stage HEPA filter even with no aerosols generated. They find the contamination has a half life of 10.8 hours which corresponds to thoron daughter decay products. This background contamination causes a significantly lower efficiency for the third HEPA filter than for the first two. They find the third stage HEPA filter has an efficiency as low as 99.5% compared to 99.98% or better for the first two HEPA filters. They attribute the lower efficiency to artifacts due to the low count rate (about 0.01 count per second) and the decay products from gaseous contaminants from radon-thoron. To mitigate these artifacts, Gonzales et al collect samples for a longer time (for entire test run of 1-2 hours), increase the decay time (a minimum of one week delay prior to counting), count the filter samples for a longer time (minimum of 17 hours), and increase the challenge aerosol concentration (four times to 10 mg/ml). Figures 20 and 21 show the resulting efficiency for the third stage HEPA filter using the original and the improved counting method.

Figure 20 shows the improved and the original test methods follow similar penetration verses concentration curves, implying that the background concentration is not materially different in the two sets of experiments. However, the challenge concentration for the improved method is substantially greater and therefore results in lower filter penetrations. In contrast, Figure 21 shows the improved test method dramatically improves the penetration verses concentration curve compared to the original test method. This indicates that the background interference is successfully reduced in the second set of experiments. The reason why the improved test method is effective in reducing the background interference in the second set of experiments and not in the first set cannot be determined from the paper (13), We recall from the previous section that the improved test methods of longer sampling time, delay time and counting time are only effective for the short life background species, not the long life species. Increasing the challenge concentration mitigates the interference from both the short life and the long life species as given by Equation 43.

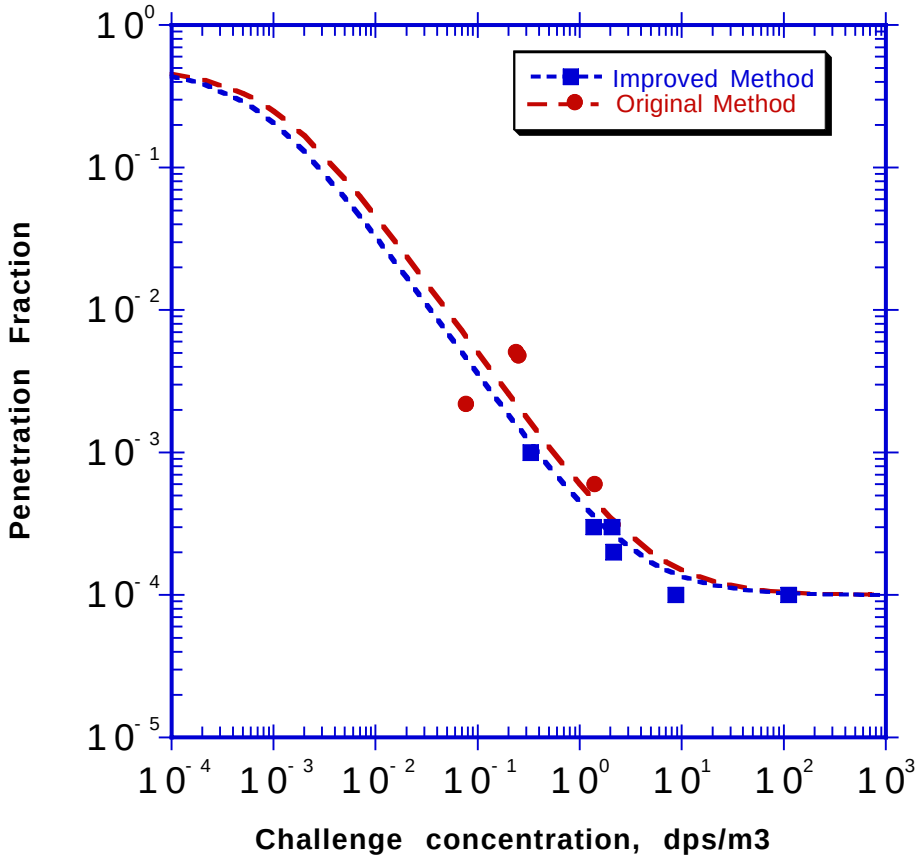

Figure 20. Efficiency of the third stage HEPA filter as a function of the activity of $^{238}PuO_2$ plus background challenging the filter for the test sequence with larger (0.7-1.6 μm) aerosols challenging the three HEPA filters in series. The improved test method of longer run times, longer count times, longer delay times, and higher challenge concentration improves the effective HEPA filter efficiency. (Gonzales et al 13)

Table 8 Parameter values used in computing the penetration curves in Figure 20 with Equation 43.

Filter Test	$P_F + P_L$	$C_{0,B}$ (dps/m3)	C_B (dps/m3)
Original	0.0001	0.001	0.0005
Improved	0.0001	0.0007	0.00035

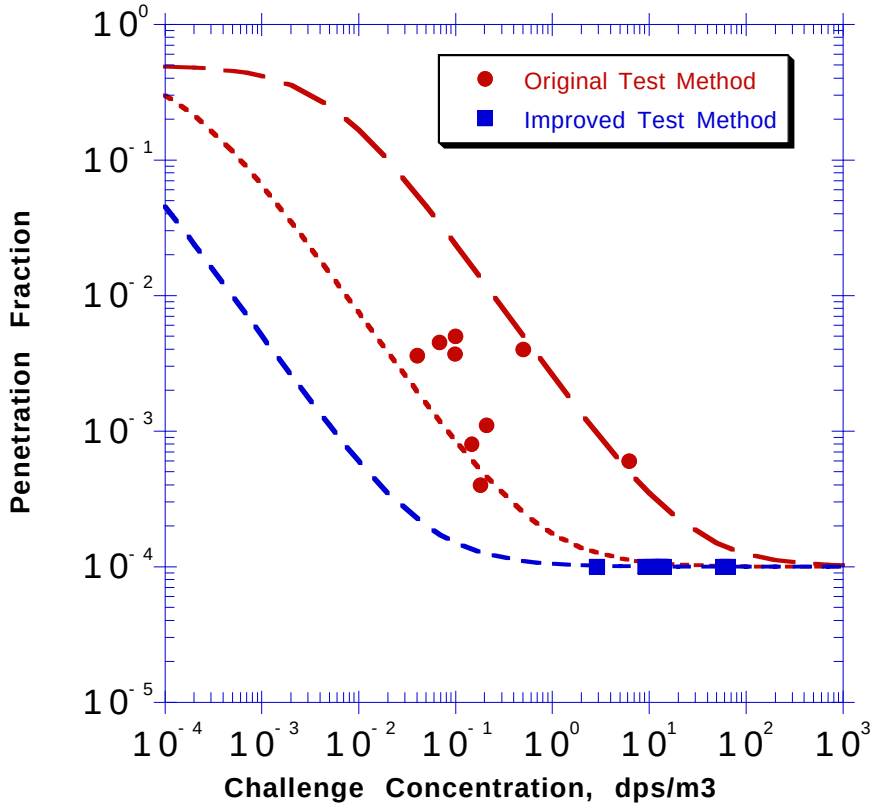

Figure 21. Efficiency of the third stage HEPA filter as a function of the air activity of $^{238}PuO_2$ exhausting the filter for the test sequence with smaller(0.3-0.5 μm) aerosols challenging the first HEPA filter. The improved test method of longer run times, longer count times, longer delay times, and higher challenge concentration improves the effective HEPA filter efficiency. (Gonzales et al 13)

Table 9. Parameters used in computing penetration curves in Figure 21 with Equation 43.

Filter Test	$P_F + P_L$	$C_{0,B}$ (dps/m3)	C_B (dps/m3)
Original A	0.0001	5E-3	2.5E-3
Original B	0.0001	1.5E-4	7.5E-5
Improved	0.0001	1E-5	5E-6

We note that the background contamination from radon-thoron daughters make a much larger contribution to the McDowell et al tests than with the Gonzales et al tests because of the much lower challenge activity, especially for the first and second HEPA filters. Moreover, McDowell et al did not allow the background radiation to decay as did Gonzales et al (13). The combination of these factors are undoubtedly responsible for the low filter efficiencies seen by McDowell et al (2).

Although there are significant experimental differences between the McDowell et al study and the Gonzales et al study, the two can be directly compared. McDowell et al place a solution of 238Pu nitrate on the first stage HEPA paper disk of 3.5 cm diameter and chemically oxidize the solution to form a Pu oxide. They then place the loaded filter in the first stage in a series of 5 filter disks and measure the amount of activity on each disk after 20 days of flowing air at 5 ft/min. In contrast, Gonzales et al generate $^{238}PuO_2$ aerosols and pass them through three stages of HEPA filters at a filter media velocity of 5 ft/min. for one to two hours.

Figure 21 shows the comparison of the McDowell et al and the Gonzales et al tests by combining the penetration curves from Figures 15, 20 and 21. For ease in comparing the two data sets, we assume the fundamental HEPA filter penetration is the same (P= 0.0001) for both studies (McDowell states the manufacturer claims the filter disks has a penetration of 0.0002). The background concentrations used in computing each of the penetration curves with Equation 43 are shown next to the curves. Also note that the challenge concentration for the McDowell et al study is computed as an effective challenge concentration based on the measured counts on the filters and the volume of air passed through the filter. From Figure 21, we see that the high filter penetration in the McDowell et al study is due to a combination of high background concentration and low challenge concentration.

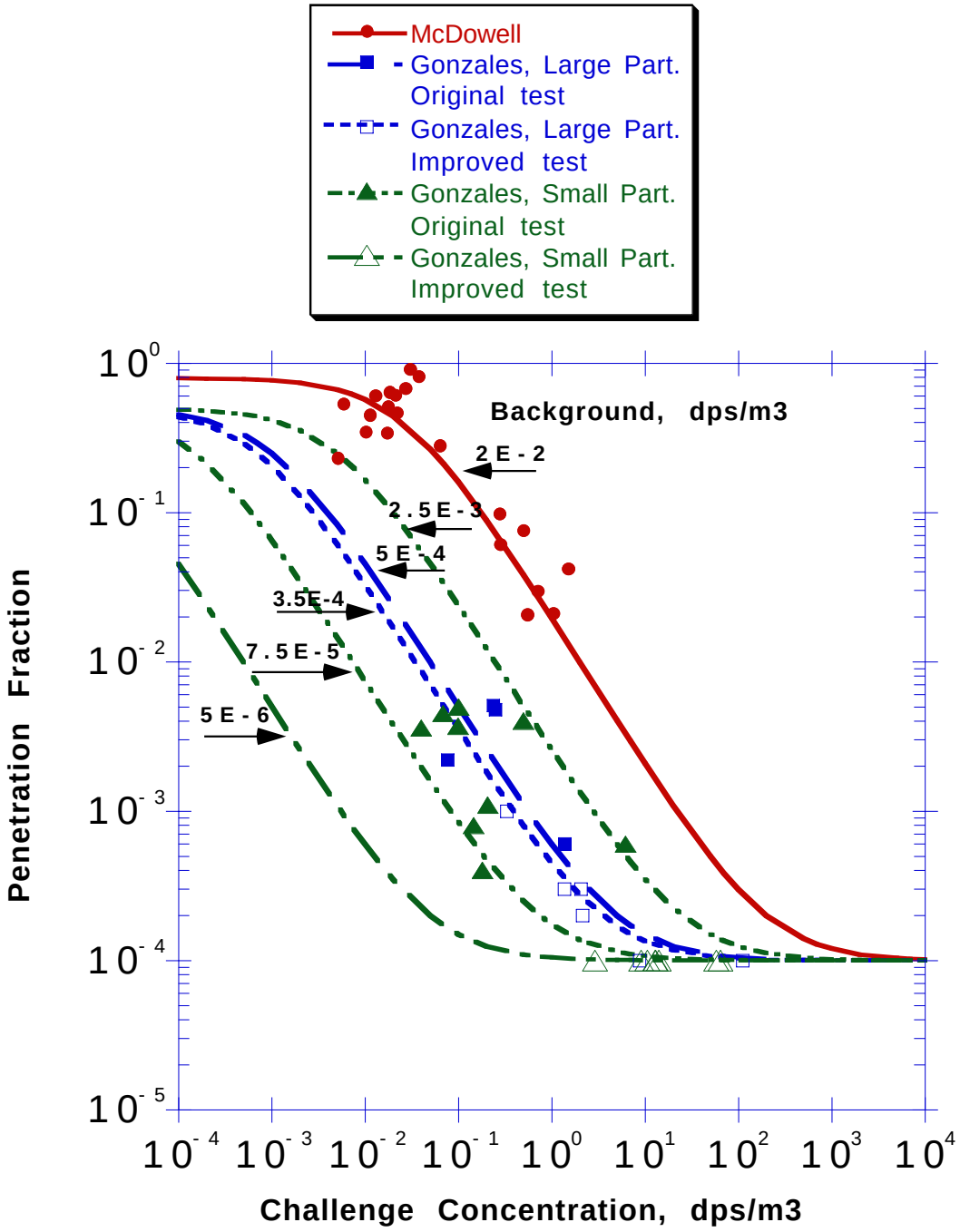

Figure 22. Comparison of McDowell et al study of 238Pu filter penetration from Figure 15 to Gonzales et al study of 238Pu penetration from Figures 20 and 21 shows the high penetration in the McDowell study is due to a high background concentration and low challenge concentration.

The data in Figure 22 is sufficient to demonstrate that the high penetration observed by McDowell at al in their tests is not due to alpha recoil but rather due to background concentration. This proof is based on the following:

(1) Gonzales et al conduct similar, but more accurate and controlled, experiments compared to McDowell et al.
(2) both studies show increased penetration over the intrinsic filter penetration.
(3) Gonzales shows the increased penetration is due to background interference by reducing the penetration with a reduction in background. McDowell has no supporting data for the alpha recoil hypothesis.
(4) Since the two studies are similar, the increased penetration in the two studies are also due to background interference. The similarity in the two experimental systems require the mechanism for the increased penetration to be the same for both experiments.

IX CONCLUSION

The efficiency of an individual HEPA filter in a multi-stage HEPA filter system is not dependent on its position. Many investigators have concluded the opposite based on experimental observations of aerosol removal efficiencies. A part of this controversy is due to the implicit assumption that the filter efficiency and the aerosol removal efficiency are equivalent. These two efficiencies are only equal if the aerosols are monodisperse. Because the filter efficiency varies strongly with particle size as seen in Figure 1, the aerosol removal efficiency for heterodisperse aerosols will differ significantly depending on the aerosol size distribution. Heterodisperse aerosols with average particle sizes much larger (or smaller) than the size of maximum filter penetration will show decreasing aerosol removal efficiencies with increasing stage of filtration as seen in Figure 5. The decreasing aerosol removal efficiency with increasing filtration stage occurs with all filter stages having the same filter efficiency.

In addition to decreasing aerosol removal efficiency with increasing filtration stage described above, other researchers suggest that the filter efficiency also decreases with filtration stage. Various mechanisms such as decreased penetration due to aerosol coagulation or increased penetration due to alpha recoil for radioactive particles are proposed to account for the observed decrease in aerosol penetration with increasing filtration stage. This report examines these experimental observations and demonstrates that the apparent decrease in HEPA filter efficiency is an artifact of the measurement and is due to background interference. The source of this artifact is the background aerosol concentration relative to the aerosol concentration that penetrates the HEPA filter. When the background is properly accounted, the efficiency of the HEPA filter does not change with each stage of filtration. A theory of filter efficiency measurements with background concentrations is developed and is in agreement with the experimental measurements.

X ACKNOWLEDGEMENT

The author is grateful to Mr. Gary Kaplan of Duke COGEMA Stone & Webster for the support that made this study possible

BIBLIOGRAPHY

(1) M.T. Ryan, W.J. McDowell, and G.N. Case, "Observations of the distribution and the nature of alpha-active particulate material in a HEPA filter used for plutonium-containing dust", Oak Ridge National Laboratory report, ORNL/TM-5765, Available from NTIS, Springfield, VA, February 1977.

(2) W.J. McDowell, F.G. Seelely, and M.T. Ryan, "Penetration of HEPA filters by alpha recoil aerosols" in Proceedings of the 14th ERDA Air Cleaning Conference, M.W. First, Editor, CONF-760822, pp 662-676., February 1977. http://tis.eh.doe.gov/hepa/

(3) N. Hetland and J. L. Russell "Adequacy of ventilation exhaust filtering system for new plutonium facilities" in Proceedings of 12th AEC Air Cleaning Conference, M.W. First, Editor, CONF-720823, pp.619-637, Oak Ridge, TN, 28-31 August, 1972, January 1973. http://tis.eh.doe.gov/hepa/

(4) N.A. Frigerio and R.S. Stowe, "Plutonium and uranium emission experience in U.S. nuclear facilities using HEPA filters" pp. 457-471, in Seminar on High Efficiency Aerosol Filtration in the Nuclear Industry, commission of the European communities, Luxmbourg, 22-25 November 1976, February 1977,

(5) J. Elder, J. Grf, J. Dewart, T. Buhl, W. Wenzel, L. Walker, and A. Stoker, "A guide to radiological accident consideratins for siting and designof DOE nonreactor nuclear facilities" Los Alamos National Laboratory Report, RFP-3650, June 1984.

(6) Atomic Energy Commission, "HEPA Filtration Guidelines" AED unpublished meeting notes, Albuquerque Operations Office, Albuquerque, NM, 1971.

(7) E. Walker, "A summary of parameters affecting the release and transport of radioactive material from an unplanned incident" Bechtel Report BNF0-81-2, September, 1978.

(8) W. Bergman, Unpublished data generated at Lawrence Livermore National Laboratory, 1997.

(9) S. Solderholm, Personal communication showing that HEPA filter efficiency curves can be fitted to log-normal size distributions, 1983

(10) E.H. Carbaugh, "A survey of HEPA filter experience" Proceedings of the17th DOE Nuclear Air Cleaning Conference, M.W. First, Editor, pp 790-800, CONF-820833, 2-5 August 1982, Denver, CO, February 1983, http://www.eh.doe.gov/hepa/

(11) W. Bergman, M.W. First, W.L. Anderson, H. Gilbert, and J.W. Jacox "Criteria for calculating the efficiency of deep-pleated HEPA filters with aluminum separators during and after design basis accidents" in Proceedings of the 23rd DOE/NRC Nuclear Air Cleaning and Treatment Conference, Buffalo, N.Y.,July 25-28, 1994, CONF-940738 , pp 563-598, February , 1995 http://www.eh.doe.gov/hepa/

(12) R. Woodard, K. Grossaint, and T. McFeetera, "Exhaust filtration on glove boxes used for aqueous processing of plutonium" in Proceedings of the 14th ERDA Nuclear Air Cleaing Conference, M.W. First, Editor, CONF-760822, pp 677-693,1977 http://www.eh.doe.gov/hepa/

(13) M. Gonzales, J.Elder and H. Ettinger, "Performance of multiple HEPA filters against plutonium aerosols" in 13th AEC Air Cleaing Conference, M.W. First, Editor, CONF-740807, San Francisco, 12-15 August 1974, pp 501-525, March 1975. http://tis.eh.doe.gov/hepa/

(14) D.A. Orth, GH. Sykes, and JM McKibben "Performance of sand filters for the separations areas at the Savannah River Plant" in Proceedings of the 16th DOE Nuclear Air Cleaning Conference, M.W. First, Editor, CONF-801038, San Diego, 20-23 October, 1980, pp 745-762, February 1981. http://tis.eh.doe.gov/hepa/

(15) D.B. Zippler, Evaluation of multistage filtration to reduce sand filter exhaust activity" in 13th AEC Air Cleaing Conference, M.W. First, Editor, CONF-740807, San Francisco, 12-15 August 1974, pp 609-619, March 1975. http://tis.eh.doe.gov/hepa/